

SURVEY AND SUMMARY

How to create state-of-the-art genetic model systems: strategies for optimal CRISPR-mediated genome editing

Yannik Bollen^{1,2,3}, Jasmin Post^{1,2}, Bon-Kyoung Koo^{4,*} and Hugo J.G. Snippert^{1,2,*}

¹Molecular Cancer Research, Center for Molecular Medicine, University Medical Center Utrecht, Utrecht University, The Netherlands, ²Oncode Institute, The Netherlands, ³Medical Cell BioPhysics, MIRA Institute, University of Twente, Enschede, The Netherlands and ⁴Institute of Molecular Biotechnology of the Austrian Academy of Sciences (IMBA), Vienna, Austria

Received January 30, 2018; Revised June 11, 2018; Editorial Decision June 11, 2018; Accepted June 14, 2018

ABSTRACT

Model systems with defined genetic modifications are powerful tools for basic research and translational disease modelling. Fortunately, generating state-of-the-art genetic model systems is becoming more accessible to non-geneticists due to advances in genome editing technologies. As a consequence, solely relying on (transient) overexpression of (mutant) effector proteins is no longer recommended since scientific standards increasingly demand genetic modification of endogenous loci. In this review, we provide up-to-date guidelines with respect to homology-directed repair (HDR)-mediated editing of mammalian model systems, aimed at assisting researchers in designing an efficient genome editing strategy.

INTRODUCTION

Mammalian model systems with defined genetic modifications are powerful tools for basic research and disease modelling. Unfortunately, precise manipulation of the mammalian genome has remained resource extensive and laborious for years, forcing many researchers to prioritize user-friendly techniques such as transgenic overexpression. The recent development of a novel generation of designer nucleases, e.g. Cas9, in combination with a better understanding of DNA repair mechanisms, is greatly improving the generation of new model systems with defined genetic modifications. Indeed, these more accurate model systems will

increasingly represent a new standard that researchers have to incorporate into their studies.

Optimal design of precise genome editing strategies is subject to many considerations that depend to a large extent on the nature of the desired modification and the cellular context in which it is pursued. While double-strand breaks (DSBs) generated by designer nucleases are sufficient to introduce deletions and rearrangements at defined genomic loci (1–3), accurate replacement or insertion of genetic material generally requires the co-introduction of a donor template that carries the modification. Moreover, the composition of the donor template can be altered to favor a particular DSB repair pathway by which the modification will be introduced into the host genome.

DSBs naturally occur during DNA replication or as a consequence of environmental factors. Fortunately, homology directed repair (HDR) pathways, e.g. homologous recombination, accurately repair DSBs by using homologous DNA as a template (4,5). Indeed, the requirement for a homologous template during HDR can be exploited to facilitate the replacement or insertion of genetic material. This mode of genome editing can be stimulated by a designer nuclease-generated DSB at the genomic locus of interest and the on-site presence of an artificial DNA template that contains (i) the new or modified genetic code and (ii) flanking regions that contain sufficient homology to the cleaved genomic strands (Figure 1). In a natural setting however, a homologous sister chromatid is only readily available to serve as a template during and shortly after DNA replication. Outside the late-S, G2 and M-phase of the cell cycle, most cells actively suppress HDR to favour non-homologous end joining (NHEJ)-mediated DSB repair (6–8). As a result, classical HDR-mediated genome edit-

*To whom correspondence should be addressed. Tel: +31 88 75 68989; Email: h.j.g.snippert@umcutrecht.nl
Correspondence may also be addressed to Bon-Kyoung Koo. Email: bonkyoung.koo@imba.oeaw.ac.at

HDR can facilitate the insertion or replacement of DNA

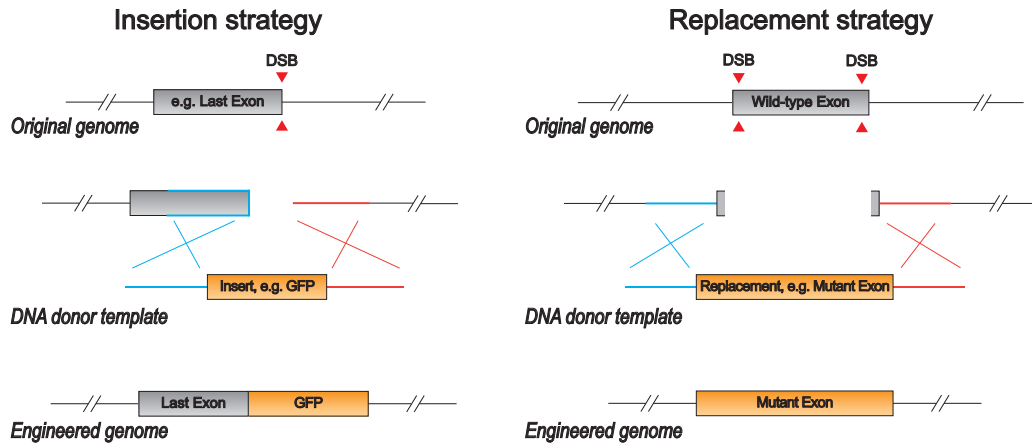


Figure 1. Exploiting HDR for insertion or replacement of DNA. Left panel: DNA Insertion strategy. A nuclease induced DSB near the stop codon triggers HDR mediated insertion of sequence in-between the homology regions of the donor template. Right panel: DNA replacement strategy. In this example, replacing an exon for a mutant variant will be accommodated via its excision by dual targeting of the nuclease to both ends of the exon (using two gRNA), followed by HDR between the DNA break extremities and the homology regions of the donor template. HDR via the 5' and 3' homology regions is indicated in blue and red respectively.

ing is largely restricted to proliferative cells (9). In contrast to HDR, NHEJ directly ligates break ends without the need of homology and is active in both proliferating and post-mitotic cells (10). NHEJ-mediated DSB repair has recently been exploited to introduce exogenous DNA into genomes of post-mitotic cells such as mature neurons and cardiac muscle cells (11,12). Along similar lines, the microhomology-mediated end joining (MMEJ) pathway can also be stimulated to facilitate precise genome editing in both proliferative and post-mitotic cells (13–15).

Although NHEJ- and MMEJ-based genome editing protocols are important innovations that enable editing in post-mitotic cells, both strategies are subject to their own set of limitations. NHEJ in particular has a tendency to generate errors during DSB repair, which may lead to inaccurate junctions during integration of the donor template (12,15). More importantly, since NHEJ ligates the cleaved genomic strands, introducing exogenous DNA (e.g. cDNA encoding fluorescent proteins) is only possible at the exact genomic location where the DSB was generated. In similar fashion, the microhomology involved in MMEJ-mediated donor integration does not tolerate significant positional divergence between the nuclease cleavage site and the desired integration site.

While mammalian genome editing via HDR remains the least error prone and most flexible strategy, traditional protocols often suffer from low editing efficiency. Fortunately, novel generations of designer nucleases and new insights into the molecular mechanisms of HDR have led to the development of more efficient HDR-mediated genome editing protocols. In this review we discuss the latest research and condense it into 'best practise guidelines' for researchers who would like to generate mammalian model systems with precisely defined genetic modifications.

DESIGNER NUCLEASES

Mouse genomes can be edited with bp-resolution using HR-mediated repair of naturally occurring DSBs in cultured ES cells (16). For decades, this procedure has been successfully used to generate new mouse models with specific integrations of exogenous DNA, so-called knock-in mouse models. Since the timing and location of DSBs could not be controlled, efficiency of HR-mediated knock-ins varied significantly between different integration-sites, e.g. genes of interest. In addition to the desired genomic modification, the donor template often included a positive selection cassette to allow selection for donor integration. Furthermore, the homology arms were extended up to 5 kb in length to increase the likelihood that the DNA template would span a naturally occurring DSB (17).

The development of designer nucleases that can target virtually all DNA loci of interest significantly enhanced the efficiency of precise genome editing, since integration of the donor template is no longer dependent on the spontaneous occurrence of a DSB near the site of interest (18). The first use-cases of designer nucleases for precise genome editing in mammalian cells involve Zinc-finger nucleases (ZFN), which were succeeded by transcription-activator like effector nucleases (TALENs) (19,20). Specificity of both ZFN and TALENs depends on a sequence-specific DNA binding domain to guide a non-specific DNA cleavage module, frequently the FokI nuclease domain. Generation of a DSB requires dual targeting in a specific spatial bi-orientation since FokI requires dimerization for nuclease activity. While ZFN and TALENs have proven effective, their usability has been limited by the requirement to pre-engineer sequence-specific DNA binding domains for each genomic target site, followed by experimental testing of nuclease activity for each ZFN or TALEN pair.

More recently, class II nucleases of the bacterial clustered regularly inter-spaced short palindromic repeats (CRISPR) adaptive immune system have been engineered to facilitate mammalian genome editing (21,22). Class II CRISPR nucleases consist of a single large monomeric nuclease with DNA target-site specificity mediated by an RNA molecule (guide RNA). Double-strand DNA cleavage occurs after sequence alignment (heteroduplex formation) between the variable region within the RNA (guide sequence) and the genomic target site. In contrast to engineering new proteins (e.g. ZFN and TALENs), these nucleases only require modification of the guide sequence to direct nuclease activity toward a specific genomic locus. In addition, the monomeric nature of class II CRISPR nucleases does not impose any orientational restraints on target sites. Potential target sites of class II CRISPR nucleases are only limited by the requirement of a protospacer adjacent motif (PAM), located either up- or downstream of the genomic target site on the strand that is not engaged in heteroduplex formation with the guide sequence (protospacer). However, most class II CRISPR nucleases have relatively permissive PAM requirements and many variants with alternate PAMs have since been validated in mammalian systems. Due to their superior properties, we will focus our discussion on two distinct types of class II CRISPR nucleases that have been adapted for mammalian genome editing to date.

CRISPR associated nuclease 9 (Cas9) is a monomeric nuclease first derived from *Streptococcus pyogenes* (SpCas9) and human codon optimized (23). Cas9 is guided by a synthetic single-guide RNA (sgRNA) of approximately 100-nucleotides (nt) in length (24), containing a 17–20 nt guide sequence that recognizes the target locus. The RuvC-like and HNH nuclease domains independently initiate cleavage on both strands 3 bp upstream of the PAM to generate a blunt-ended DSB (Figure 2A). SpCas9, the most widely used class II CRISPR nuclease, primarily recognizes the relatively permissive NGG PAM with limited activity toward NAG PAMs. Orthologs and variants of SpCas9 with alternative PAM specificities have since been published and provide an opportunity to bypass restrictions imposed by the PAM preference of conventional SpCas9 (25–34).

An interesting alternative to Cas9 is the more recently described CRISPR from *Prevotella* and *Francisella* 1 (Cpf1) (35). In addition to Cpf1 from *F. Novicida* (FnCpf1) (35,36), orthologs have been adapted from *Acidaminococcus* sp. (As-Cpf1) and *Lachnospiraceae* bacterium (LbCpf1) (37–39). There are major differences between Cas9 and Cpf1 at the molecular level (Figure 2). Cpf1 is guided by a shorter CRISPR RNA (~40 nt) and contains a guide sequence of up to 24 nt of which the 18 nt proximal to the PAM contribute most to binding and cleavage activity (40). In addition, the Cpf1 PAM is located immediately upstream of the protospacer and is T-rich. Although the exact nick positions have not been defined for all Cpf1 orthologues, DNA cleavage by Cpf1 results in a 5' staggered cut that is located away from the PAM (Figure 2B). As a consequence, small insertions or deletions (indels) generated by NHEJ-mediated repair are more likely to maintain critical target site residues, in contrast to Cas9 where indels frequently prevent re-cleavage. The additional cleavage cycles of Cpf1 were speculated to increase the probability for HDR

(35). However, a direct experimental comparison between LbCpf1 and SpCas9 in mice did not reveal a significant increase in HDR mediated donor integration when initiated by LbCpf1 (41). Whereas a more recent study in zebrafish attributed enhanced HDR by LbCpf1, among other things, to its PAM distal cleavage (42).

Specificity and cleavage efficiency of CRISPR derived nuclease variants

The specificity of designer nuclease-mediated cleavage is an important consideration since off-target cleavage can result in unintended disruption of genomic elements. Genomic cleavage by ZFN or TALEN pairs is inherently specific since it is exceedingly unlikely that two off-target sites are in the required proximity and orientation to support FokI dimerization. By contrast, the monomeric nature of type II CRISPR nucleases has raised concerns regarding off-target cleavage activity. Indeed, initial reports demonstrated substantial off-target indel generation by wild-type SpCas9 (43–46). Algorithms have since been developed that predict cleavage activity at off-target sites for type II CRISPR nucleases (43), which allows the researcher to select highly specific target sites. For particularly sensitive applications an *in vitro* analysis of off-target cleavage can be obtained via GUIDE-Seq (47).

In addition, there have been efforts to improve the intrinsic specificity of wild-type Cas9 by directed engineering of SpCas9 (26,27,48). These engineered variants display single base sensitivity at many target sites, but often sacrifice on-target cleavage efficiency when compared to wild-type SpCas9 using standard expression protocols (49). The most recent engineered SpCas9 variant, xCas9, has the most permissive PAM to date and is reported to be superior to SpCas9 in terms of specificity and on-target cleavage activity (32). However, before this variant is set to replace conventional SpCas9 it needs broader characterization.

Alternatively, the inherent specificity of FokI-based nucleases has been emulated by mutagenic inactivation of the RuvC like nuclease domain of SpCas9, thereby creating a nicking variant (25). While generating DNA nicks in close proximity on opposite genomic strands can initiate DSB repair machinery, the efficiency is generally lower compared to a DSB generated by a monomeric nuclease (21,25). Instead, Cas9 nickase variants are now increasingly used to stimulate donor integration using a single genomic DNA nick (50–53), which significantly reduces off and on-target indel generation since single DNA nicks are far less mutagenic compared to DSBs (50–52).

In addition to engineering of class II CRISPR nucleases, significant improvements in both specificity and on-target cleavage activity can be achieved by modification of the guide RNA. A truncated sgRNA of 17nt significantly enhances cleavage specificity of Cas9 (43,46,54), often without reducing on-target activity (54,55). Chemical modifications or even DNA substitutions of select sgRNA residues enhances specificity (56–59), while terminal modifications that prevent RNA degradation lead to enhanced cleavage activity (60). A combination of extensive chemical modifications throughout the sgRNA sequence further enhances Cas9 cleavage dynamics (61). Similar modifications of the Cpf1

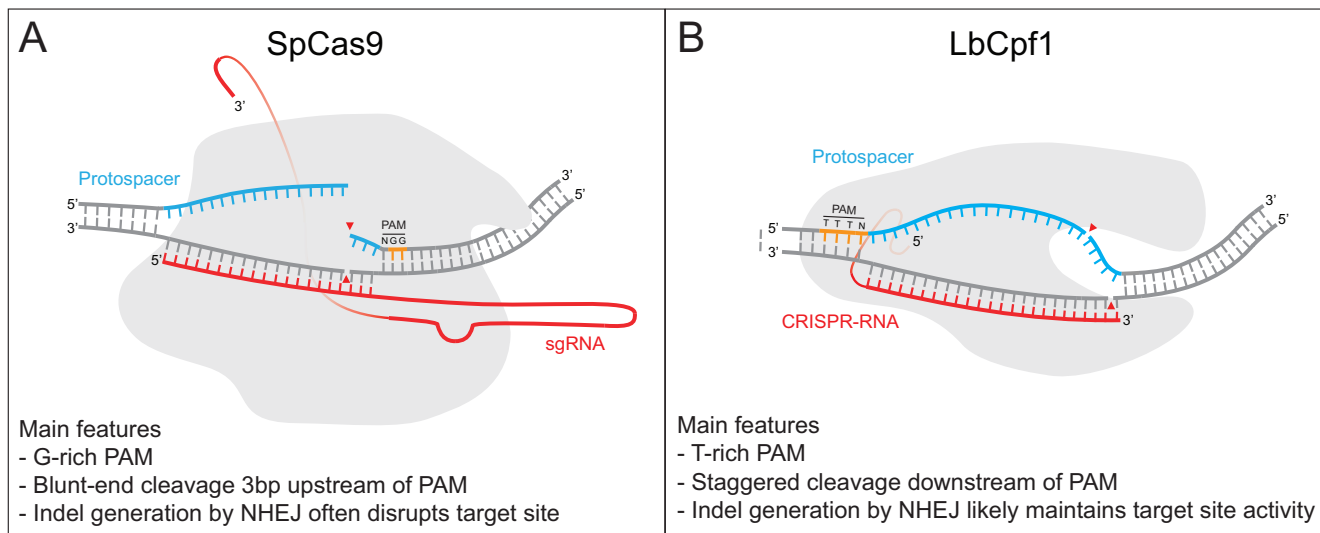


Figure 2. Key features of SpCas9 and LbCpf1. Schematic representation of SpCas9 (A) and LbCpf1 (B). Ribonucleoprotein heteroduplexed with target DNA. DNA is indicated with grey lines, unless specified otherwise (PAM and protospacer). Red lines are RNAs. Light grey shape at the back represents protein structure. DNA strand cleavage is indicated using red arrow heads.

guide RNA have also been shown to be effective (62,63). Chemically modified guide RNAs are widely available from commercial suppliers and are especially effective in combination with mRNA or ribonucleoprotein delivery of Cas9 or Cpf1, which we will discuss in a later section.

In general, most nuclease targeting approaches deal with a trade-off between on-target editing efficiency versus on-target specificity. In the interest of maximizing the efficiency of generating a new model system, we recommend a preference for established monomeric type II CRISPR nucleases (Table 1), which display the highest on-target cleavage activity. The increased off-target proclivity of monomeric nucleases is mainly a concern in the context of therapeutic *in vivo* gene correction. For research applications, careful selection of target sites will often provide sufficient specificity.

Selecting a genomic target site

While HDR mediated donor integration is maximally stimulated by a DSB at the intended integration site, additional considerations should be taken into account when selecting a genomic target site. As for target site specificity, algorithms have been developed that predict site specific cleavage activity of SpCas9 based on the nucleotide composition of the protospacer and PAM (40,64,65). Many tools are now available that implement these algorithms to score potential nuclease target sites in a selected stretch of DNA. For conventional monomeric cleavage we recommend the free CRISPR design tool offered by the Benchling platform. Among others, it predicts site specific activity of SpCas9 based on algorithms by Doench et al. (2016); allows selection of various genomes to predict specificity scores; supports a variety of PAMs including Cpf1 and allows the export of DNA oligo's suitable for ligation into commonly used expression plasmids. For a more complete overview of CRISPR design tools we suggest a review by Cui et al. (66).

In practice, the researcher will want to use a CRISPR design tool to select a nuclease target site based on the follow-

ing criteria; (i) cleavage proximity to the intended integration site; (ii) predicted on-target activity; (iii) absence of exonic off-targets with high cleavage probability and (iv) overlap with the intended integration site. The latter is preferable since a target site that overlaps with the intended integration site will be disrupted during template integration, which prevents re-cleavage without having to introduce additional point modifications in the template. In addition, although cleavage near the intended integration site is preferable, a distal target with a high on-target score may be preferred over a proximal target site with a poor on-target score. Furthermore, while a general off-target score is helpful as an overall indicator of target site specificity, predicted off-targets should be examined on an individual basis to identify off-targets that are particularly detrimental in the context of the research application. These critical sites should be screened in selected clones to confirm the absence of indels. In Figure 3, we summarize how the above criteria can be used to interpret the quality of nuclease target sites in proximity to the genomic site of integration.

In general, once CRISPR machinery becomes active within a cell, both alleles will be cleaved. Since NHEJ is dominant over HDR this often leads to the generation of indels within alleles that are not modified by HDR. Generated DSBs within an exonic region therefore often result in a heterozygous null allele in addition to the correctly modified allele. If a heterozygous null allele is detrimental to the application of the modified lineage, the modification can be introduced using a DNA nick instead of a DSB (50,52), which we will discuss in a later section. Alternatively, a DSB can be induced within the nearest intron or 3' UTR, where indels are less likely to interfere with expression or protein function. However, positional divergence between the cleavage site and the intended integration site creates an internal region of homology between the genome and donor. This promotes undesired recombination outcomes and reduces the effective probability of generating a correctly modified allele

Table 1. List of widely available monomeric type II CRISPR nucleases

Monomeric type II CRISPR nucleases	PAM	cDNA length	Reference	Addgene #
● SpCas9 (<i>S. pyogenes</i>)	NGG	4,1kb	Ran et al. 2013	62988
● SpCas9-HF1	NGG	4,1kb	Kleistiver et al. 2016	72247
● eSpCas9	NGG	4,1kb	Slaymaker et al. 2016	71814
SpCas9n(D10A)*	NGG	4,1kb	Ran et al. 2013	62987
SaCas9 (<i>S. aureus</i>)	NNGRRT	3,2kb	Ran et al. 2015	61591
SaCas9 KKH	NNNRRT	3,3kb	Kleistiver et al. 2015	70708
CjCas9 (<i>C. jejuni</i>)	NNNNRYAC	2,9kb	Kim et al. 2017	89754
FnCas9 (<i>F. novicida</i>)	YG	4,9kb	Hirano et al. 2016	68705
NmCas9 (<i>N. meningitidis</i>)	NNNGATT	3,2kb	Hou et al. 2013	47868
● xCas9**	NG	4,1kb	Hu et al. 2018	108382
● LbCpf1 (<i>Lachnospiraceae bact.</i>)	TTTN	3,7kb	Zetsche et al. 2015, Dong et al. 2016, Kim et al. 2017	84751
FnCpf1 (<i>F. novicida</i>)	KYTV	3,9kb	Zetsche et al. 2015, Tu et al. 2017	69973
AsCpf1 (<i>Acidaminococcus sp.</i>)	TTTN	3,9kb	Zetsche et al. 2015, Yamano et al. 2016, Kim et al. 2017	84750

● Recommended nuclease

● Recommended only if specificity is a special concern

● Superior targeting scope, editing efficiency and specificity relative to spCas9. Not yet broadly characterized.

Target site choice

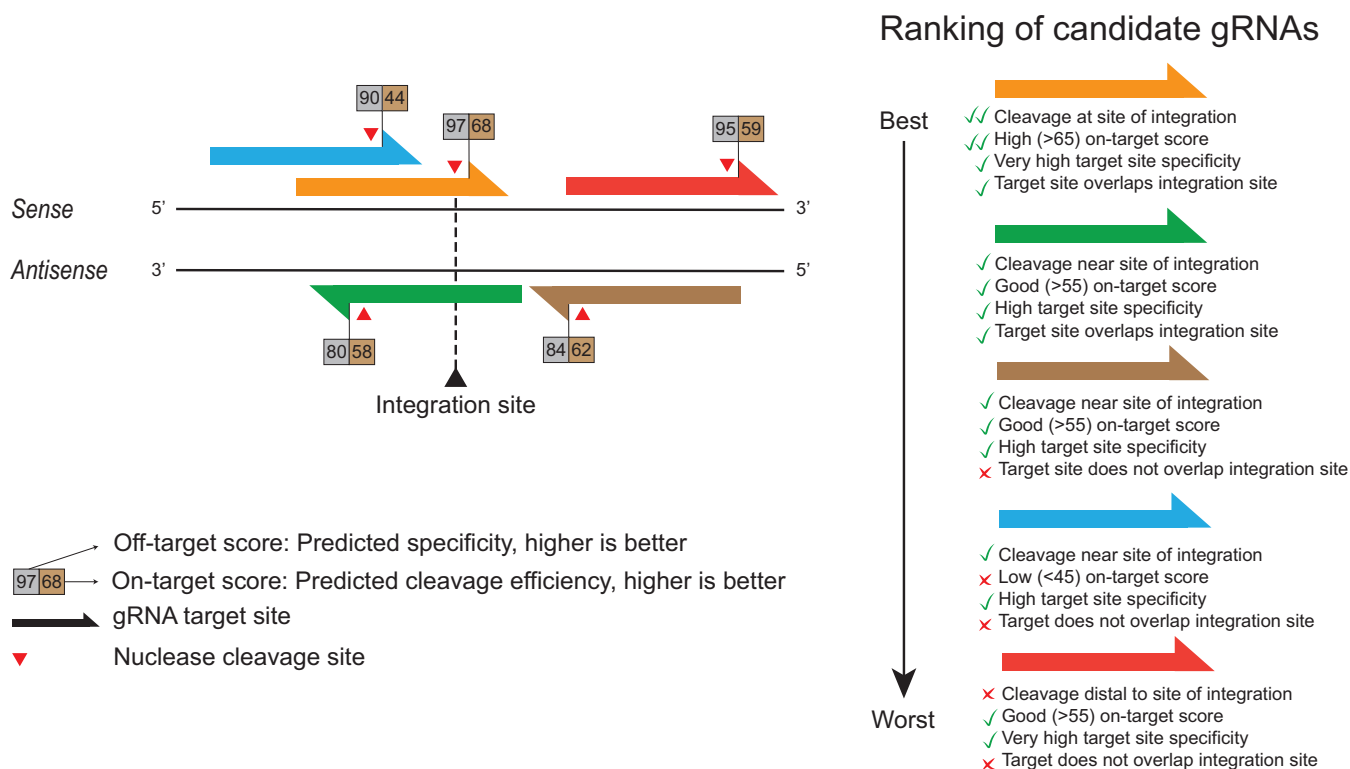


Figure 3. Nuclease target site choice. Schematic representation of a dsDNA with 5 candidate gRNA (coloured arrows). To ensure optimal HDR of a donor template at the hypothetical integration site, the possible gRNA are ranked with respect to their cleavage dynamics (on and off-target scores), as well as in relation to their location and orientation towards the intended integration site.

(Figure 4A) (67). Internal homology also occurs when two modifications are simultaneously introduced that have intervening sequences that are unmodified, for instance when generating floxed alleles with two *LoxP* sites. The probability that the modification located distal to the DSB is not incorporated increases with the extent of internal homology (68). There are two ways in which internal homology can be prevented from participating in HDR. One strategy disrupts internal homology between the donor and genome by

recoding in the corresponding region of the donor (Figure 4B) (69). Alternatively, the internal homology region can be excised from the genome by introducing two DSBs (Figure 4C) (70), which is a proven strategy when replacing a genomic sequence (71,72). However, this does increase the incidence of heterozygous null modifications by promoting the excision and inversion of alleles (67). In summary, we advocate a preference for recoding as a strategy to minimize small regions of internal homology, whereas excision might

Internal homology leads to undesired recombination events

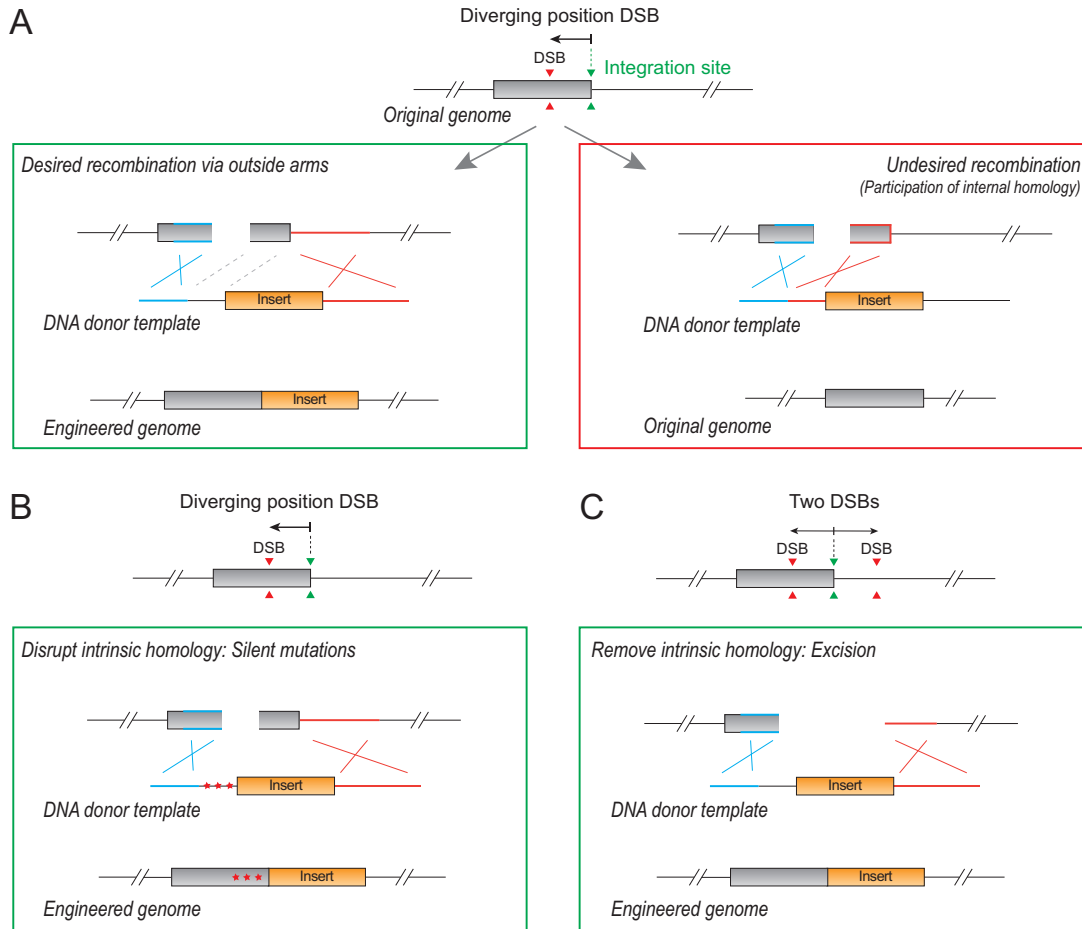


Figure 4. Internal homology increases the risk of undesired recombination events. (A) Positional divergence between DNA cleavage (DSB, indicated with red arrow heads) and the intended integration site (green arrow heads) creates the possibility for an alternative mode of recombination wherein an internal homology region participates. In the green panel, the internal homology region is indicated (dashed grey lines), but HDR is mediated via the intended homology arms at the extremities of the donor template (indicated in blue and red). Alternatively, the internal homology region (red) participates with the upstream homology arm (blue) in HDR, thereby failing to integrate the insert from the donor template (red panel). Since the size of internal homology is proportional to the probability of undesired recombination events, there are two widely used preventive strategies that minimize the extent of internal homology. (B) Internal recombination can be prevented by introducing (silent) mutations (red stars) in the internal homology region of the donor template (recoding). (C) Alternatively, in case of extensive internal homology, the region can be excised from the genome using dual targeting of the nuclease to introduce two DSBs that flank the internal homology sequence.

be best when dealing with extensive internal homology during genomic sequence replacement.

The positional divergence between the genomic integration site and the nuclease target site has to be compatible with the type of donor template that is used, since the donor needs to be capable of bridging the gap between those sites. In addition, short homology arms demand cleavage in close proximity to the intended integration site (53,73), while larger homology arms are more tolerant to distal cleavage (67). As a rule of thumb, we suggest to limit nuclease positional divergence to less than 10% of homology arm length before taking steps to counteract internal homology.

AT A GLANCE

- Monomeric type II CRISPR nucleases display the highest on-target activity and provide sufficient specificity for research applications.
- Exploring target sites for multiple monomeric Cas9 as well as Cpf1 variants increases the probability of identifying a high-quality target site.
- Cleavage proximity to the integration site and predicted on-target activity are the main parameters that researchers should use when selecting a nuclease target site to initiate HDR.
- We recommend DNA cleavage to be initiated within a distance corresponding to 10% of homology arm length with respect to the integration site.

- Internal homology between the genome and donor should be minimized, and if extensive, excised from the genome.

SELECTION STRATEGIES

Due to the relatively low success rate of accurate HDR-mediated donor integration, the end result is often a mono-allelic modification, particularly when the locus is inactive and at closed chromatin conformation (74,75). Therefore, it is important to decide in advance whether a homozygous modification is necessary. Furthermore, if a heterozygous modification is sufficient, the researcher has to consider whether perturbation of the ‘secondary’ non-recombined allele is detrimental and thus if ‘functional loss-of-heterozygosity’ needs to be prevented at all costs. Ultimately, the selection method used to identify desired clones will largely dictate the genome editing strategy as a whole. In the following paragraphs, we will discuss a variety of selection approaches and the context in which they are useful.

Direct selection for precise genetic modifications

In some cases, the desired modification conveys a phenotype that can be directly selected for. A clear example is the genomic integration of a fluorescent protein sequence that allows enrichment of correctly targeted cells via fluorescence activated cell sorting (FACS) (76). Providing that the fluorescent protein, e.g. fused to a protein of interest, will be expressed at detectable levels in the cell type of choice and that these cells are compatible with FACS. Alternatively, modifications that allow immunogenic detection, such as small epitope tags, could offer similar opportunities for FACS-based enrichment. Another class of modifications that allow direct selection are those that convey a selective advantage over the parental lineage by means of modifying culture conditions. This strategy is frequently used in the generation of oncogenic model systems since many oncogenic driver mutations activate signalling pathways that promote growth factor independency. As a result, omitting growth factors from the culture conditions enables enrichment of correctly modified cells (22,77). However, this mode of phenotypic selection risks co-selection for orthogonal oncogenic mutations that arise instead or in addition to the desired modification.

Although direct selection for the desired modification allows donor integration without additional modification of the genome, experimental settings are not always compatible with this mode of selection and may therefore require the co-integration of a genetic selection element.

Genetic selection elements

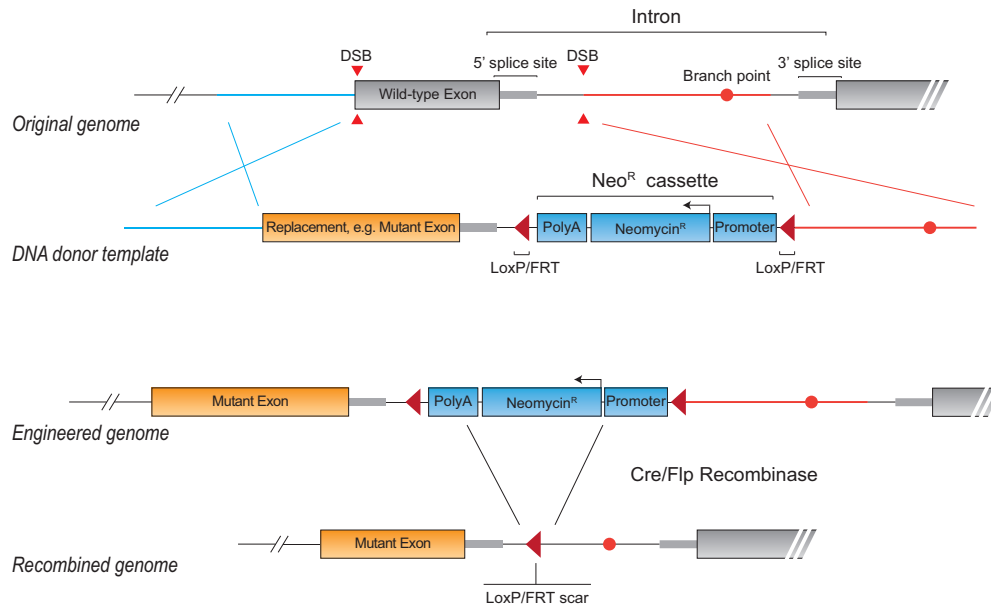
Genetic selection elements commonly drive the expression of a protein that conveys drug resistance or allows fluorescent detection to support subsequent enrichment strategies. The protein that is expressed by the selection element should be non-invasive and able to provide a selectable phenotype in the targeted cells. Expression of the selection element can either be controlled by its own independent transcriptional regulatory elements or alternatively by endogenous regulatory elements.

Independent genetic selection elements are under transcriptional control of a dedicated promoter with ubiquitous activity so that it is expressed in virtually all cell types. In addition, the cDNA that encodes the selection marker is followed by a strong PolyA transcription terminator. As a result, the cassette will function as an independent transcriptional entity. In cases where the intended genomic modification is located within an exon, the selection cassette is frequently integrated within the nearest intron (78). However, in case the last exon is targeted, e.g. to generate C-terminal fusion proteins, the element is commonly integrated within the endogenous 3’UTR of the gene of interest (79). The independent selection cassette should be integrated in close proximity to the intended genetic modification in order to minimize internal homology between the genome and donor. However, caution should be taken with respect to disruption or relocation of regulatory elements. An RNA motif prediction tool such as RegRNA 2.0 (80) can be used to determine the least invasive integration site. In addition, DNA sequences of candidate integration sites can be compared between mammalian species in order to avoid conserved regions.

The integration of an exogenous polyA transcriptional terminator upstream of the last coding exon can prematurely terminate transcription of the targeted allele (81). To prevent truncated transcription, the independent selection cassette can be integrated in the opposite transcriptional orientation with respect to the gene of interest, thereby escaping polyadenylation signal recognition by the polymerase that transcribes the targeted allele. However, integration of a strong exogenous promoter in the vicinity of endogenous regulatory elements may influence the expression level and pattern of the modified allele (16,82,83). In addition, some selection cassettes contain cryptic splice sites which may interfere with splicing of the targeted allele. (83,84). In order to minimize potential interference with endogenous expression it is good practice to remove the cassette once clones have been selected. Often this is achieved by flanking the selection cassette with either LoxP or FRT recombinase sites, allowing removal of the intervening sequence upon transient expression of the appropriate recombinase (85). This process leaves only a single recombinase site of about 30 bp in length behind, in contrast to the average size of selection cassettes of ~2 kb. Unwanted DNA sequences that are practical leftovers from the editing procedure are often referred to as a scar sequence. However, although minimal in size and widely considered intrinsically inert, the localization of the scar sequence might still interfere with expression of the modified allele (86). Scarless removal of a selection cassette can be achieved via nuclease mediated excision followed by MMEJ-based repair of appropriately designed microhomology (87) or by using the piggyBac transposase (88).

For genomic modification strategies that include a selection cassette, we recommend insertion of the cassette within a non-conserved region in-between the 5’ splice donor site and the downstream branch point (Figure 5). Insertion in-between the branch point and the 3’ splice acceptor site is not advisable since it will extend the branch sequence beyond the consensus length. When a selection cassette will be included within the endogenous 3’UTR of the locus of

Intronic integration and removal of a selection cassette



- ✓ Selection on genotype when dealing with low engineering frequency.
- ✓ No premature selection on mutation imposed phenotypes (e.g. selection for cancer mutations using modified culture conditions).
- ! Orientation and positioning of selection cassette can affect expression of the endogenous gene (problematic for essential genes).
- ! Left-over sequence after recombination (scar sequence) might not be completely inert.

Figure 5. Intronic integration and removal of a selection cassette. Schematic representation of HDR via a large DNA donor template that includes an autonomous selection cassette (in the opposite transcriptional orientation) to provide neomycin resistance. The selection cassette is integrated in the intron downstream of the integration site. Ideally the positioning of the cassette is in close proximity to the intended modification (mutant exon) to minimize internal homology. However, it is essential that sequences and relative locations of important regulatory elements for correct splicing remain intact (such as the 5' splice donor site and the 3' branch point). After clonal selection, the cassette is ideally removed from the genome in order to exclude undesired influence of the selection cassette on the expression levels of the endogenous gene. Multiple strategies exist for removal, for instance via Cre/Flp mediated recombination of LoxP or Frt sites that flank the cassette (red triangles). The minimal left-over sequence, in this case a single recombination site of ~30nt, is often referred to as a scar sequence. Scar-free removal strategies are available (see text).

interest, a less invasive location can usually be found ~50–100nt downstream of the endogenous stop codon.

As an alternative to independent expression of a selection cassette, a genetic selection element may be positioned under the transcriptional control of the endogenous allele of interest. This type of selection element does not include a promoter and polyA transcription terminator, and instead expression reflects the level and pattern of the gene of interest. The selection element is either co-integrated with an internal ribosome entry site (IRES) into the endogenous 3'UTR to become expressed as a bicistronic message (79,89), or as a C-terminal fusion protein interspaced by a ribosome skipping 2A peptide (90). It is important to realize that the stringency for selection depends in both scenarios on the activity of the endogenous promoter. Both methodologies have been successfully used in multiple studies. However, insertion of an IRES sequence into the endogenous 3'UTR may influence expression levels (91), presumably by altering mRNA stability, while C-terminal 2A peptide fusion leaves the endogenous 3'UTR intact. On the

other hand, the relative positioning of an IRES within the 3'UTR is flexible while C-terminal 2A peptide fusion requires integration immediately upstream of the endogenous stop codon. Furthermore, while the translational efficiency of an IRES might substantially deviate from the expression levels of the upstream gene, the newest generation of 2A fusion peptides generate near equimolar protein ratios. Therefore, 2A peptide reporters are more suitable as a readout of expression levels (90). On the other hand, a downside of the 2A peptides is the addition of a 19–22 amino acid peptide at the C-terminus of the upstream protein, which can potentially interfere with normal protein function.

Sampling-based selection

Direct selection for correct template integration is convenient via the simultaneous integration of a genomic selection element. However, this is not always necessary or even preferable. Foremost, using a genomic selection element requires construction of a larger donor even if the de-

sired modification is only a single base substitution. Moreover, scarless removal of a selection cassette remains laborious to engineer, often requiring negative selection strategies. Sampling-based selection is an alternative strategy to identify desired clones. Although broadly applicable, this approach is especially helpful when generating delicate disease models that require solitary integration of their respective mutation. Sampling-based selection generally involves enrichment for cells that obtained transient expression of the designer nuclease. A common strategy relies on FACS-based enrichment of transfected cells via co-expression of 2A-GFP (92) or the use of fluorescently labelled tracrRNA (93). Alternatively, if the cell line is not compatible with FACS, transient puromycin selection can be used instead (94). When integrating epitope tags and other small modifications, the frequency of correctly modified clones can be estimated within the bulk population using TIDER, an adaptation of the popular TIDE algorithm which decomposes Sanger sequencing data generated from multiple alleles (95,96). This will provide the researcher with an impression of the number of clones that need to be screened in order to obtain a correctly modified clone. In the next section we will discuss the use of TIDER or PCR-based strategies to determine the zygosity state of the modified alleles within individual clones.

We recommend sampling-based selection for modifications that are compatible with ssDNA donor design since these can often be integrated with relatively high efficiency. We advise against sampling-based selection when: (i) integrating large DNA donor templates that often suffer from low integration efficiencies; (ii) when working with model systems that are relatively laborious to maintain and scale and (iii) when the projected editing efficiency is low.

Screening clones using PCR-based strategies.

Once clones are obtained they have to be screened to confirm correct editing and determine the zygosity of the modified alleles. A straightforward strategy involves the design of primer pairs that are able to discriminate between non-integrated (*wild-type*) and correctly modified alleles. For insertion strategies, this requires a PCR that spans the genomic integration site with at least one primer annealing to endogenous DNA sequences outside the homology arm regions (Figure 6A). This approach prevents false positive amplicons in cases where the donor template randomly integrated into the genome. The generated PCR amplicon allows discrimination of wild-type and insertion alleles based on product size. If a clone generates amplicons corresponding to both wild-type and insertion alleles this indicates heterozygosity, whereas the absence of a wild-type amplicon indicates homozygosity. If the integrated sequence is so large that a corresponding amplicon would preclude efficient genomic PCR amplification, a secondary primer can be designed which anneals only to the integrated DNA sequence.

If a genomic sequence is to be replaced, a PCR spanning the corresponding region often allows discrimination between wild-type and replacement alleles based on product size. In cases where both amplicons are of similar size (wild-type and mutant), primer sets should be designed that am-

plify either wild-type or mutant specific amplicons (Figure 6B).

While a single primer set is often able to identify zygosity, we recommend the design of redundant primer sets since genomic PCR's can be challenging. In addition, PCR amplicons should span the entire modified sequence so that the integrity of correctly modified alleles can be confirmed via DNA sequencing of the amplicons. The absence of indels within the non-recombined wild-type allele can be analysed by decomposing the Sanger sequencing data using TIDE, or alternatively by sub-cloning the amplicon into cloning vectors prior to individual Sanger sequencing of multiple clones representing single alleles.

AT A GLANCE

- Genomic modifications that do not allow direct selection may require co-introduction of a genetic selection element, expressed either as an independent transcriptional entity or under control of an endogenous promoter.
- Removal of a genetic selection element is crucial to minimize potential artefacts.
- Sampling-based selection is a broadly applicable alternative to genomic selection cassettes and is recommended for modifications that are compatible with ssDNA donor design.
- A single genomic PCR is often able to discriminate between wild-type and modified alleles based on amplicon size.

DONOR COMPOSITION

DNA donor templates can consist of synthesized single-stranded oligodeoxyribonucleotide (ssODN) donors, larger ssDNA fragments, plasmid- or viral-based donor vehicles, and PCR amplified double-stranded (ds)DNA donors. Each donor type offers distinct advantages and has a unique demand for the extent and distribution of homology. In general, the donor type that is best suited for the introduction of a particular modification depends on the size of the modification, but also on the selection strategy that can be used.

ssDNA donors

Efficient ssDNA donor integration via HDR pathways can be stimulated by a DSB or DNA nick(s) (53,71). The compact nature of ssDNA donors results in a relatively high concentration of donor molecules within each cell, which is thought to enhance the probability of alignment between the donor and target locus (52). Indeed, precise editing efficiency is generally higher when mediated by ssDNA donors as compared to plasmid-based donor vectors (21). Moreover, editing efficiency increases proportionally with donor concentration (97).

Commercially synthesized ssODN donors allow efficient integration of modifications up to ~60 nt during synthesis-dependent strand annealing (SDSA) mediated repair of Cas9 induced DSBs (53). The proposed mechanism of SDSA is relevant for this discussion. It involves: (i) 5' end resection of the cleaved genomic strands and subsequent base pairing with the 3' arm of the ssODN; (ii) extension of the

PCR based identification of correctly modified alleles

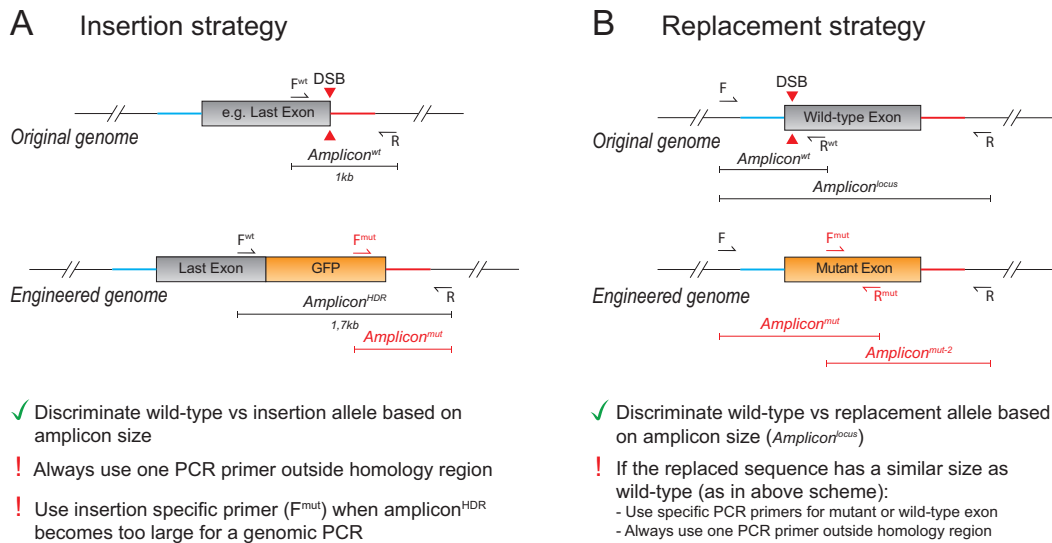


Figure 6. PCR-based identification of correctly modified alleles. PCR-based assays can be employed to expedite screening of clones for correctly modified alleles (A). For insertion strategies, zygosity can be determined by discrimination between PCR amplicon sizes spanning the integration site. Subsequently, sequence integrity can be confirmed by sequencing of the amplicons. (B) Discrimination based on size is not always possible when replacing DNA sequences with modified versions. Sequence specific primers can be used to generate amplicons that are specific for WT or modified alleles.

genomic sequence using the ssODN as a template and (iii) capture of the opposite genomic strand by the newly synthesised homology (69). Many studies have contributed to optimal design parameters for ssODN donors in conjunction with blunt-end DNA cleavage, which we summarized in Figure 7A. Work by Richardson *et al.* initially suggested that ssODN polarity (i.e. ssODN in sense or antisense orientation) should be complementary to the strand that is not heteroduplexed with Cas9 (52). However, this finding has not been consistent with subsequent studies (42,98,99). Paix *et al.* propose an alternative model where ssODN polarity should be adjusted such that base pairing between the 3' arm of the ssODN and the genomic strand is not interrupted by the intended modifications (69). As a consequence, optimal ssODN polarity depends on the relative position of the generated DSB in relation to the integration site. If the DSB is generated downstream of the intended integration site then a sense ssODN should be preferred, whereas cleavage upstream of the integration site favours an antisense ssODN. The polarity rule by Paix *et al.* is in agreement with the performance of ssODNs in the study by Richardson *et al.* and with other published work (52,98,99). In addition to polarity, the length and distribution of homology should be considered. Richardson *et al.* proposed that the 5' arm has a greater demand for homology (52). This asymmetric distribution of homology has been confirmed in an independent study by Liang *et al.* (98). In addition, while in a study by Guo *et al.* an asymmetric ssODN underperformed, we note that the asymmetric ssODN had an unfavourable polarity according to Paix *et al.* while the symmetric ssODN had the correct polarity, which may explain the underperformance of the asymmetric ssODN (99). We therefore recommend ssODN polarity according to Paix *et al.* with an asymmetric distribution of homology of 30–

36 nt at the 3' and 67–91 nt at the 5' of the ssODN according to Richardson *et al.* Finally, the stability of the ssODN, and thus the editing efficiency, is significantly enhanced by phosphorothioate (PS) modifications of the last two nucleotide bonds at both the 3' and 5' end (98), which can be included during commercial synthesis. Collectively, these design rules have been established using Cas9 mediated cleavage although they will likely translate to Cpf1 mediated cleavage as well.

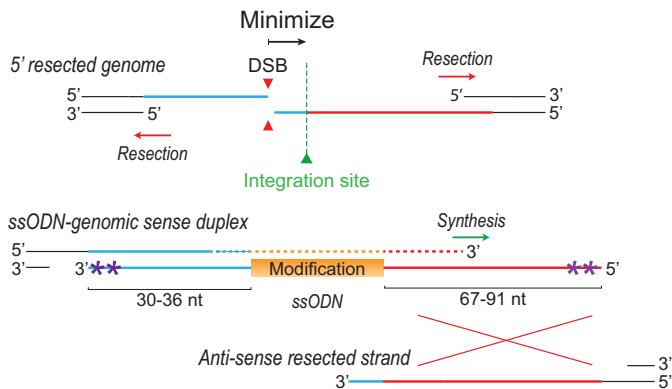
We recommend the use of ssODNs for the precise generation of modifications ranging from single nucleotide insertions or deletions to small epitope tags and multi-codon deletions. When a single ssODN is used to introduce two or more modifications that are spaced apart, the intervening region should be recoded using silent mutations (69). As a consequence the entire region between the proximal and distal modifications is likely treated as a single region of heterology (53). Although this might negatively impact overall integration efficiency, it will favour simultaneous incorporation of all modifications since internal homology is prevented (53,69).

If a single point mutation is desired we strongly encourage the researcher to explore whether a base-editor is applicable. Base-editors trigger nucleotide-conversion after being targeted to specific genomic loci based on their fusion to catalytically-dead or nickase Cas9. As a result, base-editors can efficiently mediate any single nucleotide substitution without genomic cleavage (100–102).

Since base-editors do not rely on cleavage, no indel mutations are introduced within the secondary allele, keeping its coding sequence intact and preventing 'functional loss-of-heterozygosity'. As such, base-editors are optimal for introducing heterozygous point mutations, like oncogenic mutations. Similarly, two or more nucleotide substitutions can

Parameters for design of DNA donor templates

A Optimized ssODN design

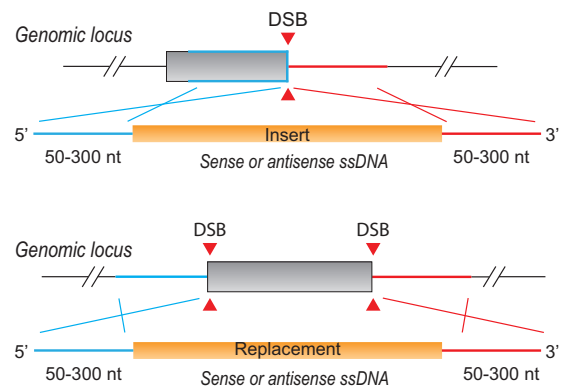


* Phosphorothioate bond

! Ensure that modifications do not interfere with annealing of the 3' end of the ssODN and a 3' genomic overhang
 - When cutting downstream of the integration site use sense polarity
 - When cutting upstream of the integration site use antisense polarity (as in above scheme)

✓ Modifications up to ~50 nt

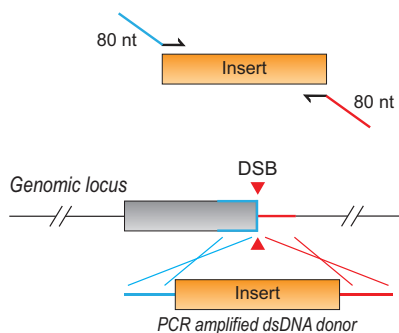
B Long ssDNA design



✓ Integration of commercially generated ssDNA up to ~2kb in length

! Certain DNA complexities may be rejected by commercial suppliers (e.g. high GC content)

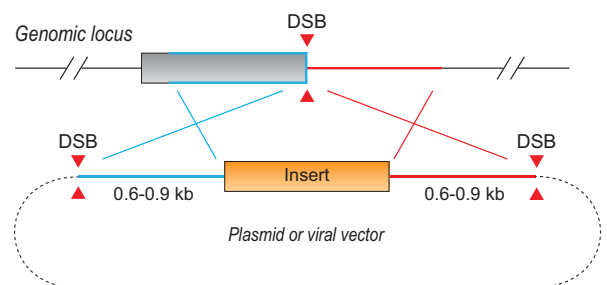
C PCR amplified dsDNA donor design



✓ Include up to 80nt homology arms as overhangs on the PCR primers

✓ Relatively cheap and low-tech generation of donor template

D Targeting vector design



✓ Donor template excision by flanked nuclease target sites (identical to genomic target site)
 - Compatible with in-trans paired nicking when using DNA nickase

✓ Suitable for modifications >2 kb in length

! Use homology arms up to 2 kb when not flanked by nuclease target sites (traditional design)

Figure 7. Parameters for donor template design. (A) Schematic representation of ssODN template integration stimulated by a DSB (red arrow heads). Due to 5' DNA end resection by DNA repair pathway associated proteins, an ssODN can be designed to either hybridize in the sense or antisense orientation. Complete hybridization from the 3' end of the ssODN towards the DNA strand extremity (DSB site) is advised. In this example, ssODN hybridization with the antisense genomic resected overhang (red) would lead to mismatches, whereas hybridization with the sense overhang (blue) does not. Furthermore, homology should be distributed in an asymmetric fashion in favour of the 5' homology arm. Phosphorothioate bonds prevent ssODN degradation. (B) Schematic representation of HDR using long ssDNA templates. (C) Schematic representation of HDR using PCR amplified dsDNA donor. Homology arms up to 80nt can be added to conventional PCR primers as 3' overhangs. (D) Schematic representation of HDR using a donor vector. Vectors can be assembled as complex donor templates from multiple sources. Flanking of the template with nuclease target sites identical to the genomic target site allows excision and linearization of the template concurrent with genomic cleavage.

be integrated without compromising the secondary allele by stimulating ssODN mediated editing via a DNA nick (52,53). Although polarity of the ssODN with respect to the generated nick determines the preferred HDR pathway, it has little influence on editing efficiency. Moreover, while optimal ssODN composition for this mode of nick editing has not been determined, an ssODN with 77 nt homology arms was integrated at roughly half the efficiency when stimulated by a DNA nick as compared to a DSB (53).

Commercial ssDNA is now available up to 2 kb, which allows highly efficient generation of modifications that previously required construction of a dedicated donor vector (72,103,104). Precise genome editing by long ssDNA donors is likely mediated by the single-strand annealing pathway instead of SDSA. As such, the optimal design parameters for long ssDNA donors are likely to be different from ssODN design and have yet to be fully determined. Nevertheless, efficient editing is achieved with homology arms of 50–300 nt with no clear preference for a particular polarity of the ssDNA (Figure 7B). We highly recommend long ssDNA donors for modifications that are too large for ssODN synthesis. The only exceptions are current size restrictions and sequence complexities that are rejected by commercial suppliers, such as high GC content.

PCR generated dsDNA donors

Commercial synthesis of long ssDNA can be expensive and when performed ‘in-house’ requires construction of a vector with an appropriately located T7 promoter (104). A PCR generated dsDNA donor is a cheap alternative which is especially useful for medium sized insertions that allow direct selection, e.g. fluorescent knock-in alleles. Homology arms up to 80 nt (or even longer via a nested PCR) can be appended to the desired insertion as overhangs in the PCR primers (Figure 7C) (105–107). The integration efficiency observed for PCR-generated donors is similar to that of traditional donor vectors (108).

Plasmid or viral donor vectors

Modifications that are too large for ssDNA synthesis require construction of a viral or plasmid-based donor vector using molecular cloning techniques. Since a substantial part of these vectors consists of backbone elements such as bacterial selection cassettes or viral packaging sequences, the effective donor template concentration per cell is disproportionately reduced compared to ssDNA donors. On the other hand, donor vectors have sufficient capacity to include a genomic selection cassette, making absolute editing efficiency less important.

Traditionally, donor vectors required relatively large homology arms of up to 2 kb in order facilitate efficient HR mediated donor integration by a designer nuclease-generated DSB (67,108). Homology arm length of donor vectors can be reduced to 0.6–0.9 kb by flanking the donor with nuclease target sites that are identical to the genomic target site (Figure 7D). As a consequence, a linear donor supply is liberated concurrent with genomic cleavage (108,109). The linear nature and relatively long homology arms of the excised donor fragment is thought to stimulate a novel HDR pathway, termed homology-mediated end

joining (109). Currently, no direct negative consequences of in-vivo donor excision have been reported, and since nuclease target sites are easily included as overhangs in the PCR amplification of the homology arms, the construction of this type of dual-cut donor vector does not require extra labor. Moreover, a donor vector that is flanked with nuclease target sites is compatible with a novel strategy called in trans paired nicking (50), where concurrent nicking of the genome and donor triggers efficient integration without genomic cleavage. However, it remains unclear whether this strategy can trigger replacement of genomic sequence.

We expect donor vectors flanked with nuclease target sites to develop into the preferred strategy for the integration or substitution of large transgenic elements. Since the homology arms of these vectors are relatively short, vector construction and subsequent genotyping is far more convenient when compared to the use of traditional donor vectors with longer homology arms.

AT A GLANCE

- Due to the absence of backbone sequences ssDNA donors result in a high effective donor concentration which improves editing efficiency.
- Modifications up to ~60 nt can be integrated using ssODN donors. Optimized ssODNs are constructed with an asymmetric distribution of homology and a polarity determined by the position of the DSB relative to the intended integration site.
- Modifications up to 1.9 kb can be integrated using commercially available long ssDNA donors.
- PCR generated donors with short homology arms allow cost efficient generation of fluorescent knock-in alleles.
- Modifications too large for ssDNA donor templates require vector construction. By flanking the donor with nuclease target sites the homology demand can be reduced to 0.6–0.9 kb.

DELIVERY OF HDR COMPONENTS

Efficient delivery of genome editing components into target cells is a crucial step in the process towards generation of genetically modified model systems. The delivery method should be matched to the model system of choice and to the manner in which the designer nuclease and donor are presented to the cell.

In vitro delivery

To date, most publications involving precise CRISPR-mediated genome editing have used established transfection methods including liposomal transfection, electroporation and peptide-mediated cell penetration, to deliver nuclease expression constructs and donor templates into target cells (23,110–113). Although generally robust and broadly applicable, plasmid delivery has particular drawbacks that should be considered. Foremost, the introduction of high concentrations of foreign DNA into cells can trigger an immune response in certain cell types, which can eventually lead to programmed cell death (114). In addition, prolonged expression of nucleases from plasmid DNA increases the

frequency of indel mutations at off-target sites (115,116) and along similar lines, prolonged stability of plasmid DNA increases the probability of random plasmid integration into the genome. To circumvent these issues, nucleases can be delivered as pre-assembled ribonucleoprotein complexes (RNPs) or as mRNA molecules along with *in vitro* transcribed or commercially synthesized gRNA (115,117,118). Messenger RNA is significantly less stable compared to plasmid DNA, resulting in a relatively short but robust spike of nuclease activity. Similarly, RNP delivery circumvents translation, resulting in an immediate spike of nuclease activity followed by a rapid decline due to protein degradation. In each case, nuclease activity is short lived, which reduces the probability of generating off-target indels. Furthermore, the immediate spike in nuclease activity ensures co-presence with initial high concentrations of DNA donor templates prior to their degradation. Indeed, RNP delivery in particular is associated with a significant increase in precise genome editing efficiency (98,119). In addition, since assembly of RNPs or delivery of mRNA is compatible with chemically modified gRNA, these protocols open up new avenues of maximizing editing efficiency.

Some cell lineages, such as primary cells, remain difficult to transfect with classical transfection methods. Instead, these cells are often virally transduced (120). However, the cargo restrictions of many viral vectors often prohibit CRISPR mediated genome editing applications. BacMam technology, which employs baculoviral vectors that have the capacity to carry large DNA cargo up to 38 kb in length (121), has recently been used to address viral cargo issues. All the components required to support CRISPR-mediated precise integration of large DNA constructs, including the donor template itself, can be integrated within a single baculoviral genome (122,123). In addition, transduction in mammalian cells occurs in a transient manner by default, thereby minimizing the risk of viral integration into the host genome. However, since viral transduction is associated with general safety risks, alternative transfection methods are under continuous development (124,125).

While common *in vitro* plasmid delivery methods have been widely applicable in mono-layer cell cultures, transfection of 3D organoid cultures is more challenging. Although both transfection and electroporation can successfully deliver plasmids in organoid structures, the resulting transfection efficiency is generally low (77,110,111). An optimized electroporation protocol has demonstrated significantly improved transfection efficiency in comparison to liposomal transfection (111). Nevertheless, cell viability post transfection generally remains low and consequently large quantities of organoid-derived cells are required in order to obtain successfully edited clones. Alternatively, human intestinal organoids have been virally transduced to deliver CRISPR machinery, however this method is not compatible with ssDNA donor delivery (123).

To conclude, delivery of nuclease expression constructs following conventional protocols is convenient for less demanding applications such as heterozygous modifications that allow direct selection. RNP delivery, in particular when assembled with enhanced chemically modified gRNA, supports highly efficient precise editing in conjunction with ssDNA donors (71,98), and more recently in combination

with AAV donor transduction (126). Therefore, we encourage the use of RNP delivery protocols whenever applicable, and especially when generating modifications that depend on a sampling-based selection approach. In this regard, enrichment of an RNP transfected population can be achieved by assembling RNPs with fluorescent tracrRNA (93). Finally, cell lines that are particularly difficult to transfect can usually be virally transduced. In this regard, viral-based delivery of genome editing components may be useful as a platform for the precise incorporation of a particular modification across many different cell lines of the same organism.

In vivo delivery

Although significant progress has been made in the development of *in vitro* delivery protocols that target a cellular population in its completeness, *in vivo* delivery is far more challenging. Initial publications demonstrated proof-of-principle *in vivo* HDR-mediated genome editing in adult mice using non-viral hydrodynamic tail vein injections, co-delivering Cas9-sgRNA expression constructs and ssODN donor template into the liver (127,128). However, among other things due to inferior delivery methods, HDR-mediated gene editing efficiency remained very low. The sporadic introduction of cancer mutations *in vivo* for the rapid development of human cancer models in mice has mainly been supported by locally injected lentiviral transduction (129,130). Further development of these protocols may benefit from the latest generation of high-capacity adenoviral vectors that are able to carry both the nuclease and gRNA scaffolds in one viral particle (131).

The ultimate clinically-related goal of highly efficient genome editing is to correct disease mutations and phenotypes in living patients in terms of personalized medicine. In contrast to *in vitro* culture systems that allow clonal selection and outgrowth of successfully modified cells, most disease phenotypes for which *in vivo* genome editing is considered a potential clinical break-through require mutational correction in a large fraction of cells that manifest the diseased phenotype. Delivery methods to accommodate this level of precise nuclease mediated editing are currently out of reach. In addition, since many genetic conditions are caused by single point mutations, base editors are a far more likely candidate for clinical translation. Since the scope of our review is to facilitate guidelines for researchers that would like to genetically engineer their preferred model system, we refer to a number of excellent reviews with respect to *in vivo* genome editing for clinical applications (132–134).

AT A GLANCE

- Plasmid based nuclease delivery is convenient for less demanding applications such as heterozygous modifications that allow direct selection.
- We encourage the use of RNP delivery protocols in conjunction with chemically modified gRNA, especially when depending on a sampling-based selection approach.
- BacMam technology is recommended for the generation of large genomic modifications in difficult to transfect cell lines, since it allows the delivery of all HDR components in a single construct.

- Clinical applications of CRISPR-mediated precise gene correction are currently out of reach.

COMPLEMENTARY STRATEGIES TO ENHANCE PRE-CISE EDITING EFFICIENCY

In addition to optimized donor template design, nuclease choice, genomic target site selection and delivery, there are additional complementary strategies that may further enhance CRISPR-mediated HDR efficiency. A major focus has been the development of tools to suppress the competing NHEJ repair pathway. Strategies include depletion or inhibition of the NHEJ pathway proteins KU70, KU80 and DNA ligase IV using either shRNAs (107,135), Adenovirus 4 (Ad4) proteins (135), or molecular inhibition of DNA ligase IV via small molecule inhibitors such as SCR7 (107,135–138). Similar to observations in DNA ligase IV-deficient flies, depletion or inhibition of DNA ligase IV reduced NHEJ activity, while increasing HDR in both mouse and mammalian cell lines (135,136,139). A similar effect was observed upon the depletion of the KU complex (137). NHEJ pathway suppression may be of particular interest when generating homozygous mutations, as the Ad4 protein-induced degradation of DNA ligase IV enhanced the net yield of homozygous clones when used in combination with selection markers (135). However, significant care should be taken when using the SCR7 compound, as it can enhance the number of off-target integrations and induces cell toxicity when used at high concentrations. Also, the sensitivity to NHEJ inhibition seems to be cell type specific, as improvements in HDR efficiency varied significantly between cell lines and often does not result in a notable beneficial effect (107,108,136). The search for compounds that enhance HDR continues. One study demonstrated resveratrol to be an even more potent enhancer of HDR-mediated genome editing efficiency when compared to SCR7 (138), albeit the molecular mechanism governing its therapeutic properties remain elusive (140). In addition, two new compounds that enhance Cpf1-mediated HDR have recently been identified (141).

Another interesting approach is cell cycle synchronization in combination with timed Cas9 RNP delivery to focus nuclease activity to the G2/M-phase of the cell cycle when HDR is dominant. Indeed, cell cycle synchronization prior to Cas9 RNP delivery resulted in a significant increase in HDR efficiency in a variety of cell types (8,97,108). As expected, this also reduced the frequency of NHEJ events (108). In addition, the minimal concentration of Cas9 RNPs and donor DNA for sufficient HDR was substantially lower (8,97). However, cell cycle inhibitors by themselves may significantly affect cell viability, thereby decreasing the effective number of targetable cells in the population (8). In addition, several reports demonstrated that combining NHEJ inhibition and cell cycle synchronization did not further improve HDR efficiency, suggesting that HDR is already the predominant repair pathway during the G2/M-phase (8).

Several reports have investigated the effect of temperature on nuclease mediated HDR. For instance, cold shock treatment at 32°C for 24–48 h post transfection was shown to enhance Cas9 mediated HDR in human induced pluripotent

stem cells (99). However, a similar protocol turned out to be detrimental to Cas9 induced HDR in many other human cell types (142). A relative heat shock to 34°C in zebrafish significantly enhanced Cpf1 mediated HDR but had no effect on Cas9 mediated HDR (42). Collectively these results suggest that the effect of temperature on HDR rates requires further investigation before it should be generally applied.

Although complementary strategies are useful in the context of maximizing precise editing efficiency we advise against using these strategies by default. Rather, they should be used in parallel or as a back-up plan when initial genome editing strategies yielded an insufficient number of clones.

AT A GLANCE

- Inhibition of NHEJ, either via co-expression of Adenovirus 4 proteins or via small molecule inhibitors of DNA ligase IV, can enhance HDR-mediated genome editing.
- Cell cycle synchronization in the G2/M-phase combined with timed RNP delivery induces nuclease activity in the HDR dominant phase of the cell cycle.
- Complementary strategies should not be used by default but rather in parallel or as a backup strategy.

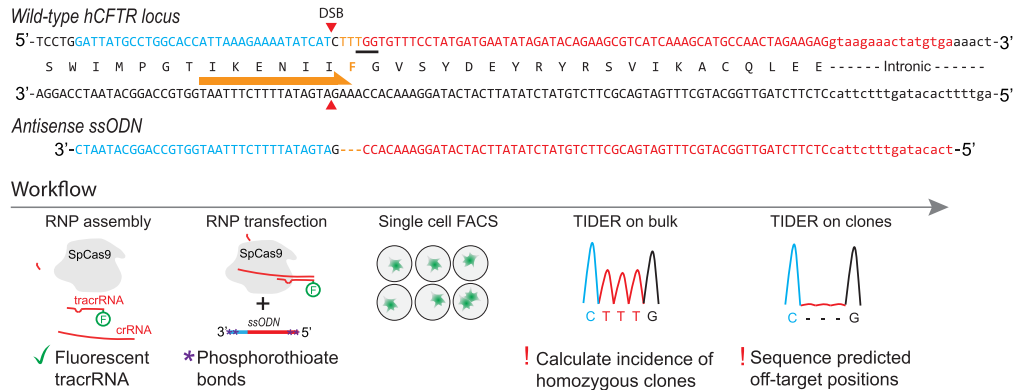
DISCUSSION

In the last couple of years, CRISPR-mediated genome editing has evolved at a very rapid pace. The expansion of the CRISPR-associated toolkit and our increased understanding of the molecular mechanisms that govern HDR have improved our ability to accurately edit mammalian genomes. Whereas many reviews have shed light on the historical and molecular background of CRISPR technology, up-to-date guidelines with respect to the design of HDR-mediated genome editing strategies were lacking. This review aims to function as a decision-making guide to assist researchers in using state-of-the-art genetics to generate mutant variants of their model system. It should be of special interest to classical cell biologists and biochemists without extensive genetic backgrounds. Especially in 2D cell cultures, introducing disease-related point mutations or protein fusions at endogenous loci is highly efficient. Indeed, solely relying on transient overexpression of (mutant) effector proteins is no longer recommended since scientific standards increasingly demand genetic modifications at endogenous loci. However, we stress the importance of a well thought out genome editing strategy in advance, since the entire process from design to a validated model system may still require a couple of months work. To summarize the current knowledge, opportunities and strategic options available to researchers, we will discuss three different design examples where many aspects discussed in this review will be placed into a real context.

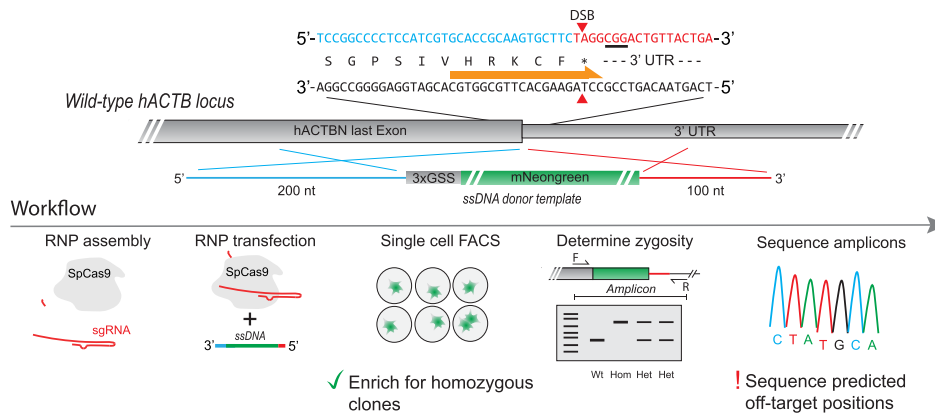
Example 1 (Figure 8A): Homozygous loss of phenylalanine at position 508 of the Cystic Fibrosis transmembrane conductance regulator (CFTR) is the most frequent genetic variant that causes Cystic Fibrosis (143). An accurate human model system will require homozygous deletion of $\Delta F508$ without additional genetic scarring. The small size and homozygous nature of the deletion strongly favours an

Genome editing design examples

A ΔF508 hCFTR disease model lineage in a 2D cell line



B hACTB-mNeogreen C-terminal knock-in in a 2D cell line



C hKRT20-CreERT2 in colon organoids

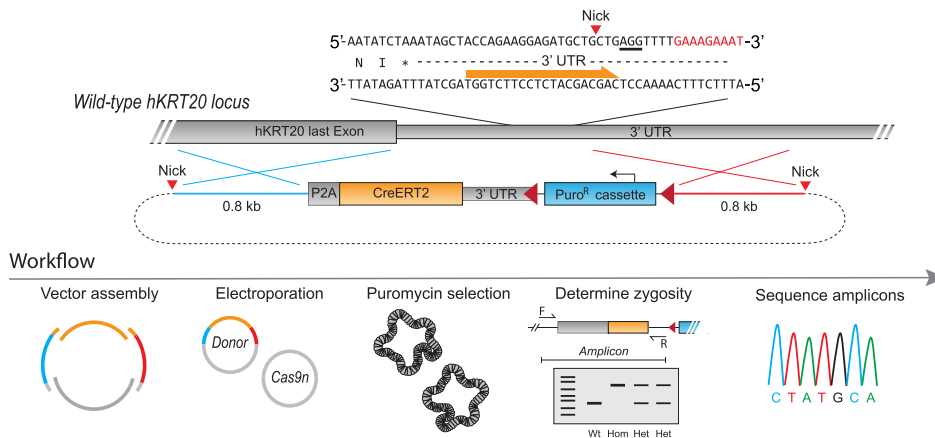


Figure 8. Designing genome editing strategies: 3 real examples. **(A)** Schematic workflow of the practical steps and the sequence information for the process of generating ΔF508 CFTR mutant cell lines. Top: The dsDNA sequence of the *CFTR* gene is presented around the intended modification site. In between the corresponding amino acid sequence is depicted. As a donor template, an asymmetric antisense ssODN is advised (see text). **(B)** Schematic workflow of the practical steps and the sequence information for the process of generating an mNeogreen knock-in at the C-terminus of hACTB in cell lines. Top: The dsDNA sequence of the *hACTB* gene is presented around its endogenous stop codon. The corresponding amino acid sequence is depicted in between the dsDNA. An ssDNA donor template is depicted below the schematic representation of the *hACTB* locus. Rationale for strategy design is described in the text. **(C)** Schematic workflow of the practical steps and the sequence information for the process of generating a CreERT2 knock-in in the *hKRT20* locus via a P2A fusion at its C-terminus in human colon organoids. Top: A stretch of dsDNA sequence of the 3'UTR of the *hKRT20* gene is presented. Below the locus is a schematic representation of the donor plasmid. Rationale for strategy design is described in the text. Yellow arrow indicates gRNA. Cleavage sites (DSB) are indicated with red arrow heads. PAM sequences are underscored.

ssODN donor. A SpCas9 target site is available that cleaves just one nucleotide upstream of the deletion site, favouring an antisense ssODN designed with an asymmetric distribution of homology. Since deletion of $\Delta F508$ will destroy the Cas9 target site, no additional silent mutations are required within the donor. Although the selected target site has a poor predicted on-target efficiency, better performing target sites cleave further away from the deletion site, likely leading to an overall decrease in performance when working with an ssODN. In addition, no well positioned CpfI target sites are available. RNP transfection will maximize editing efficiency, which enhances the isolation of homozygous clones. Since direct selection for $\Delta F508$ CFTR is not available, RNPs will be assembled with chemically stabilized fluorescent tracrRNA in combination with commercially synthesized and chemically stabilized CRISPR-RNA containing the guide sequence. Fluorescent tracrRNA allows FACS-based single cell sorting of transfected cells. In addition, isolating a bulk population for TIDER analysis will give an estimate for the frequency of homozygous clones.

Example 2 (Figure 8B): Overexpression of fluorescent fusion proteins illuminates cell biology at the costs of altering protein homeostasis and potentially protein function. In contrast, endogenous tagging of the respective genes is potentially less invasive and probably truer to nature. Fluorescent beta-actin (ACTB) fusions are popular in cell biology (144). In order to insert mNeongreen (a bright monomeric green fluorophore (145)) at its C-terminus in a human cell line, we selected a highly active SpCas9 target site that cleaves within the stop codon of ACTB. The mNeongreen coding sequence will be fused in frame to the C-terminus of hACTB via a 3xGSS flexible linker (144), thereby also disrupting the selected SpCas9 target site. Considering the size of the modification, integration efficiency is maximized by using an ssDNA donor. About 100 nt downstream of the stop codon, the 3' UTR runs into a stretch of sequence complexity which commercial suppliers currently reject. We therefore limited the length of the 3' homology arm of the sense ssDNA donor to 100 nt. By contrast, 5' homology is more flexible which we extended to 200 nt, providing an extra buffer against 5' degradation. The nature of the modifications allows direct selection by FACS and may even permit enrichment for homozygous clones if desired. Correct integration of the template, as well as its zygosity, can easily be determined using a single PCR that spans the integration site. In addition, an additional primer set can be designed with one primer placed on top of the nuclease cleavage site to facilitate identification of heterozygous clones where the secondary allele remained intact.

Example 3 (Figure 8C): Patient-derived organoids recapitulate the stem cell driven differentiation hierarchy of self-renewing tissues, among others enabling the study of lineage differentiation (146). Unfortunately, genetic modification of organoids via sampling-based selection is often prohibited by poor transfection efficiency and laborious clonal expansion. In addition, when modifying a gene that is exclusively expressed in a terminally differentiated cell state, many direct selection strategies are problematic. A C-terminal P2A-CreERT2 fusion to Keratin 20 (KRT20) allows genetic lineage tracing within the enterocyte lineage of human colon organoids (147). In order to select for this C-terminal fu-

sion, a selection cassette is integrated within the 3' UTR at an unconserved position. The orientation of the selection cassette is not important in this instance since the cassette will be removed using Flp-mediated recombination in an undifferentiated population of cells. Due to the size of the modification (~ 4 kb) and sequence complexity of the selection cassette, donor vector construction is required. During assembly of the donor vector, both homology arms should be flanked by a copy of the genomic target sequence. This approach will enable both in trans paired nicking as well as linear donor excision concurrent with genomic cleavage. While the relative position of the selection cassette with respect to CreERT2 creates a limited stretch of internal homology between the endogenous 3'UTR and the donor template, we recommend against introducing point mutations within the start of the 3' UTR in order to avoid disruption of potential regulatory motifs. Instead, we minimize homology by placing the cassette in close proximity to the last exon.

Innovative genome editing technologies will continue to be developed, thereby constantly modifying and changing existing editing procedures and methods. A recent innovation is RNP-donor conjugates that aim to deliver the DNA donor template directly at the site of nuclease activity (148,149). In addition, assembly of donor vectors by molecular cloning may soon be unnecessary as better ssDNA synthesis protocols are being developed (150). Ultimately, considering the progression toward nick-mediated editing and base-editors, we anticipate that the future of complex genome editing might not even involve nuclease activity at all.

FUNDING

Funding for open access charge: Core lab funding.

Conflict of interest statement. None declared.

REFERENCES

- Blasco,R.B., Karaca,E., Ambrogio,C., Cheong,T.C., Karayol,E., Minero,V.G., Voena,C. and Chiarle,R. (2014) Simple and rapid in vivo generation of chromosomal rearrangements using CRISPR/Cas9 technology. *Cell Rep.*, **9**, 1219–1227.
- Song,Y., Yuan,L., Wang,Y., Chen,M., Deng,J., Lv,Q., Sui,T., Li,Z. and Lai,L. (2016) Efficient dual sgRNA-directed large gene deletion in rabbit with CRISPR/Cas9 system. *Cell Mol. Life Sci.*, **73**, 2959–2968.
- Wolfs,J.M., Hamilton,T.A., Lant,J.T., Laforet,M., Zhang,J., Salemi,L.M., Gloor,G.B., Schild-Poulter,C. and Edgell,D.R. (2016) Biasing genome-editing events toward precise length deletions with an RNA-guided TevCas9 dual nuclease. *Proc. Natl. Acad. Sci. U.S.A.*, **113**, 14988–14993.
- Chapman,J.R., Taylor,M.R. and Boulton,S.J. (2012) Playing the end game: DNA double-strand break repair pathway choice. *Mol. Cell*, **47**, 497–510.
- Pfeiffer,P., Goedecke,W. and Obe,G. (2000) Mechanisms of DNA double-strand break repair and their potential to induce chromosomal aberrations. *Mutagenesis*, **15**, 289–302.
- Saleh-Gohari,N. and Helleday,T. (2004) Conservative homologous recombination preferentially repairs DNA double-strand breaks in the S phase of the cell cycle in human cells. *Nucleic Acids Res.*, **32**, 3683–3688.
- Heyer,W.D., Ehmsen,K.T. and Liu,J. (2010) Regulation of homologous recombination in eukaryotes. *Annu. Rev. Genet.*, **44**, 113–139.

8. Yang, D., Scavuzzo, M.A., Chmielowiec, J., Sharp, R., Bajic, A. and Borowiak, M. (2016) Enrichment of G2/M cell cycle phase in human pluripotent stem cells enhances HDR-mediated gene repair with customizable endonucleases. *Sci. Rep.*, **6**, 21264.
9. Chan, F., Hauswirth, W.W., Wensel, T.G. and Wilson, J.H. (2011) Efficient mutagenesis of the rhodopsin gene in rod photoreceptor neurons in mice. *Nucleic Acids Res.*, **39**, 5955–5966.
10. Rothkamm, K., Kruger, I., Thompson, L.H. and Lobrich, M. (2003) Pathways of DNA double-strand break repair during the mammalian cell cycle. *Mol. Cell Biol.*, **23**, 5706–5715.
11. Maresca, M., Lin, V.G., Guo, N. and Yang, Y. (2013) Obligate ligation-gated recombination (ObLiGaRe): custom-designed nuclease-mediated targeted integration through nonhomologous end joining. *Genome Res.*, **23**, 539–546.
12. Suzuki, K., Tsunekawa, Y., Hernandez-Benitez, R., Wu, J., Zhu, J., Kim, E.J., Hatanaka, F., Yamamoto, M., Araoka, T., Li, Z. *et al.* (2016) In vivo genome editing via CRISPR/Cas9 mediated homology-independent targeted integration. *Nature*, **540**, 144–149.
13. Nakade, S., Tsubota, T., Sakane, Y., Kume, S., Sakamoto, N., Obara, M., Daimon, T., Sezutsu, H., Yamamoto, T., Sakuma, T. *et al.* (2014) Microhomology-mediated end-joining-dependent integration of donor DNA in cells and animals using TALENs and CRISPR/Cas9. *Nat. Commun.*, **5**, 5560.
14. Sakuma, T., Nakade, S., Sakane, Y., Suzuki, K. T. and Yamamoto, T. (2016) MMEJ-assisted gene knock-in using TALENs and CRISPR-Cas9 with the PITCh systems. *Nat. Protoc.*, **11**, 118–133.
15. Yao, X., Wang, X., Liu, J., Hu, X., Shi, L., Shen, X., Ying, W., Sun, X., Wang, X., Huang, P. *et al.* (2017) CRISPR/Cas9-mediated precise targeted integration in vivo using a double cut donor with short homology arms. *EBioMedicine*, **20**, 19–26.
16. Muller, U. (1999) Ten years of gene targeting: targeted mouse mutants, from vector design to phenotype analysis. *Mech. Dev.*, **82**, 3–21.
17. Hasty, P., Rivera-Perez, J. and Bradley, A. (1991) The length of homology required for gene targeting in embryonic stem cells. *Mol. Cell Biol.*, **11**, 5586–5591.
18. Storic, F., Durham, C.L., Gordenin, D.A. and Resnick, M.A. (2003) Chromosomal site-specific double-strand breaks are efficiently targeted for repair by oligonucleotides in yeast. *Proc. Natl. Acad. Sci. U.S.A.*, **100**, 14994–14999.
19. Urnov, F.D., Miller, J.C., Lee, Y.L., Beausejour, C.M., Rock, J.M., Augustus, S., Jamieson, A.C., Porteus, M.H., Gregory, P.D. and Holmes, M.C. (2005) Highly efficient endogenous human gene correction using designed zinc-finger nucleases. *Nature*, **435**, 646–651.
20. Miller, J.C., Tan, S., Qiao, G., Barlow, K.A., Wang, J., Xia, D.F., Meng, X., Paschon, D.E., Leung, E., Hinkley, S.J. *et al.* (2011) A TALE nuclease architecture for efficient genome editing. *Nat. Biotechnol.*, **29**, 143–148.
21. Cong, L. and Zhang, F. (2015) Genome engineering using CRISPR-Cas9 system. *Methods Mol. Biol.*, **1239**, 197–217.
22. Drost, J., van Jaarsveld, R.H., Ponsioen, B., Zimmerlin, C., van Boxtel, R., Buijs, A., Sachs, N., Overmeer, R.M., Offerhaus, G.J., Begthel, H. *et al.* (2015) Sequential cancer mutations in cultured human intestinal stem cells. *Nature*, **521**, 43–47.
23. Jinek, M., East, A., Cheng, A., Lin, S., Ma, E. and Doudna, J. (2013) RNA-programmed genome editing in human cells. *Elife*, **2**, e00471.
24. Jinek, M., Chylinski, K., Fonfara, I., Hauer, M., Doudna, J.A. and Charpentier, E. (2012) A programmable dual-RNA-guided DNA endonuclease in adaptive bacterial immunity. *Science*, **337**, 816–821.
25. Ran, F.A., Hsu, P.D., Lin, C.Y., Gootenberg, J.S., Konermann, S., Trevino, A.E., Scott, D.A., Inoue, A., Matoba, S., Zhang, Y. *et al.* (2013) Double nicking by RNA-guided CRISPR Cas9 for enhanced genome editing specificity. *Cell*, **154**, 1380–1389.
26. Kleinstiver, B.P., Pattanayak, V., Prew, M.S., Tsai, S.Q., Nguyen, N.T., Zheng, Z. and Joung, J.K. (2016) High-fidelity CRISPR-Cas9 nucleases with no detectable genome-wide off-target effects. *Nature*, **529**, 490–495.
27. Slaymaker, I.M., Gao, L., Zetsche, B., Scott, D.A., Yan, W.X. and Zhang, F. (2016) Rationally engineered Cas9 nucleases with improved specificity. *Science*, **351**, 84–88.
28. Guilinger, J.P., Thompson, D.B. and Liu, D.R. (2014) Fusion of catalytically inactive Cas9 to FokI nuclease improves the specificity of genome modification. *Nat. Biotechnol.*, **32**, 577–582.
29. Kleinstiver, B.P., Prew, M.S., Tsai, S.Q., Nguyen, N.T., Topkar, V.V., Zheng, Z. and Joung, J.K. (2015) Broadening the targeting range of Staphylococcus aureus CRISPR-Cas9 by modifying PAM recognition. *Nat. Biotechnol.*, **33**, 1293–1298.
30. Hirano, H., Gootenberg, J.S., Horii, T., Abudayyeh, O.O., Kimura, M., Hsu, P.D., Nakane, T., Ishitani, R., Hatada, I., Zhang, F. *et al.* (2016) Structure and Engineering of Francisella novicida Cas9. *Cell*, **164**, 950–961.
31. Hou, Z., Zhang, Y., Propson, N.E., Howden, S.E., Chu, L.F., Sontheimer, E.J. and Thomson, J.A. (2013) Efficient genome engineering in human pluripotent stem cells using Cas9 from Neisseria meningitidis. *Proc. Natl. Acad. Sci. U.S.A.*, **110**, 15644–15649.
32. Hu, J.H., Miller, S.M., Geurts, M.H., Tang, W., Chen, L., Sun, N., Zeina, C.M., Gao, X., Rees, H.A., Lin, Z. *et al.* (2018) Evolved Cas9 variants with broad PAM compatibility and high DNA specificity. *Nature*, **556**, 57–63.
33. Ran, F.A., Cong, L., Yan, W.X., Scott, D.A., Gootenberg, J.S., Kriz, A.J., Zetsche, B., Shalem, O., Wu, X., Makarova, K.S. *et al.* (2015) In vivo genome editing using Staphylococcus aureus Cas9. *Nature*, **520**, 186–191.
34. Kim, E., Koo, T., Park, S.W., Kim, D., Kim, K., Cho, H.Y., Song, D.W., Lee, K.J., Jung, M.H., Kim, S. *et al.* (2017) In vivo genome editing with a small Cas9 orthologue derived from Campylobacter jejuni. *Nat. Commun.*, **8**, 14500.
35. Zetsche, B., Gootenberg, J.S., Abudayyeh, O.O., Slaymaker, I.M., Makarova, K.S., Essletzbichler, P., Volz, S.E., Joung, J., van der Oost, J., Regev, A. *et al.* (2015) Cpf1 is a single RNA-guided endonuclease of a class 2 CRISPR-Cas system. *Cell*, **163**, 759–771.
36. Tu, M., Lin, L., Cheng, Y., He, X., Sun, H., Xie, H., Fu, J., Liu, C., Li, J., Chen, D. *et al.* (2017) A ‘new lease of life’: Fncpf1 possesses DNA cleavage activity for genome editing in human cells. *Nucleic Acids Res.*, **45**, 11295–11304.
37. Dong, D., Ren, K., Qiu, X., Zheng, J., Guo, M., Guan, X., Liu, H., Li, N., Zhang, B., Yang, D. *et al.* (2016) The crystal structure of Cpf1 in complex with CRISPR RNA. *Nature*, **532**, 522–526.
38. Yamano, T., Nishimasu, H., Zetsche, B., Hirano, H., Slaymaker, I.M., Li, Y., Fedorova, I., Nakane, T., Makarova, K.S., Koonin, E.V. *et al.* (2016) Crystal structure of Cpf1 in complex with guide RNA and target DNA. *Cell*, **165**, 949–962.
39. Li, B., Zeng, C. and Dong, Y. (2018) Design and assessment of engineered CRISPR-Cpf1 and its use for genome editing. *Nat. Protoc.*, **13**, 899–914.
40. Kim, H.K., Song, M., Lee, J., Menon, A.V., Jung, S., Kang, Y.M., Choi, J.W., Woo, E., Koh, H.C., Nam, J.W. *et al.* (2017) In vivo high-throughput profiling of CRISPR-Cpf1 activity. *Nat. Methods*, **14**, 153–159.
41. Zhang, Y., Long, C., Li, H., McAnally, J.R., Baskin, K.K., Shelton, J.M., Bassel-Duby, R. and Olson, E.N. (2017) CRISPR-Cpf1 correction of muscular dystrophy mutations in human cardiomyocytes and mice. *Sci. Adv.*, **3**, e1602814.
42. Moreno-Mateos, M.A., Fernandez, J.P., Rouet, R., Vejnar, C.E., Lane, M.A., Mis, E., Khokha, M.K., Doudna, J.A. and Giraldez, A.J. (2017) CRISPR-Cpf1 mediates efficient homology-directed repair and temperature-controlled genome editing. *Nat. Commun.*, **8**, 2024.
43. Hsu, P.D., Scott, D.A., Weinstein, J.A., Ran, F.A., Konermann, S., Agarwala, V., Li, Y., Fine, E.J., Wu, X., Shalem, O. *et al.* (2013) DNA targeting specificity of RNA-guided Cas9 nucleases. *Nat. Biotechnol.*, **31**, 827–832.
44. Cradick, T.J., Fine, E.J., Antico, C.J. and Bao, G. (2013) CRISPR/Cas9 systems targeting beta-globin and CCR5 genes have substantial off-target activity. *Nucleic Acids Res.*, **41**, 9584–9592.
45. Mali, P., Aach, J., Stranges, P.B., Esvelt, K.M., Moosburner, M., Kosuri, S., Yang, L. and Church, G.M. (2013) CAS9 transcriptional activators for target specificity screening and paired nickases for cooperative genome engineering. *Nat. Biotechnol.*, **31**, 833–838.
46. Fu, Y., Foden, J.A., Khayter, C., Maeder, M.L., Reyon, D., Joung, J.K. and Sander, J.D. (2013) High-frequency off-target mutagenesis induced by CRISPR-Cas nucleases in human cells. *Nat. Biotechnol.*, **31**, 822–826.
47. Tsai, S.Q., Zheng, Z., Nguyen, N.T., Liebers, M., Topkar, V.V., Thapar, V., Wyvekens, N., Khayter, C., Iafrate, A.J., Le, L.P. *et al.* (2015) GUIDE-seq enables genome-wide profiling of off-target cleavage by CRISPR-Cas nucleases. *Nat. Biotechnol.*, **33**, 187–197.

48. Kulcsar, P.I., Talas, A., Huszar, K., Ligeti, Z., Toth, E., Weinhardt, N., Fodor, E. and Welker, E. (2017) Crossing enhanced and high fidelity SpCas9 nucleases to optimize specificity and cleavage. *Genome Biol.*, **18**, 190.
49. Kim, S., Bae, T., Hwang, J. and Kim, J.S. (2017) Rescue of high-specificity Cas9 variants using sgRNAs with matched 5' nucleotides. *Genome Biol.*, **18**, 218.
50. Chen, X., Janssen, J.M., Liu, J., Maggio, I., t Jong, A.E.J., Mikkers, H.M.M. and Goncalves, M. (2017) In trans paired nicking triggers seamless genome editing without double-stranded DNA cutting. *Nat. Commun.*, **8**, 657.
51. Nakajima, K., Zhou, Y., Tomita, A., Hirade, Y., Gurumurthy, C.B. and Nakada, S. (2018) Precise and efficient nucleotide substitution near genomic nick via noncanonical homology-directed repair. *Genome Res.*, **28**, 223–230.
52. Richardson, C.D., Ray, G.J., DeWitt, M.A., Curie, G.L. and Corn, J.E. (2016) Enhancing homology-directed genome editing by catalytically active and inactive CRISPR-Cas9 using asymmetric donor DNA. *Nat. Biotechnol.*, **34**, 339–344.
53. Kan, Y., Ruis, B., Takasugi, T. and Hendrickson, E.A. (2017) Mechanisms of precise genome editing using oligonucleotide donors. *Genome Res.*, **27**, 1099–1111.
54. Fu, Y., Sander, J.D., Reyon, D., Cascio, V.M. and Joung, J.K. (2014) Improving CRISPR-Cas nuclease specificity using truncated guide RNAs. *Nat. Biotechnol.*, **32**, 279–284.
55. Singh, K., Evens, H., Nair, N., Rincon, M.Y., Sarcar, S., Samara-Kuko, E., Chuah, M.K. and VandenDriessche, T. (2018) Efficient in vivo liver-directed gene editing using CRISPR/Cas9. *Mol. Ther.*, **26**, 1241–1254.
56. Ryan, D.E., Taussig, D., Steinfeld, I., Phadnis, S.M., Lunstad, B.D., Singh, M., Vuong, X., Okochi, K.D., McCaffrey, R., Olesiak, M. et al. (2018) Improving CRISPR-Cas specificity with chemical modifications in single-guide RNAs. *Nucleic Acids Res.*, **46**, 792–803.
57. Yin, H., Song, C.Q., Suresh, S., Kwan, S.Y., Wu, Q., Walsh, S., Ding, J., Bogorad, R.L., Zhu, L.J., Wolfe, S.A. et al. (2018) Partial DNA-guided Cas9 enables genome editing with reduced off-target activity. *Nat. Chem. Biol.*, **14**, 311–316.
58. Cromwell, C.R., Sung, K.R., Park, J., Kryslar, A.R., Jovel, J., Kim, S.K. and Hubbard, B.P. (2018) Incorporation of bridged nucleic acids into CRISPR RNAs improves Cas9 endonuclease specificity. *Nat. Commun.*, **9**, 1448.
59. Kartje, Z.J., Barkau, C.L., Rohilla, K.J., Ageely, E.A. and Gagnon, K.T. (2018) Chimeric guides probe and enhance Cas9 biochemical activity. *Biochemistry*, **57**, 3027–3031.
60. Hendel, A., Bak, R.O., Clark, J.T., Kennedy, A.B., Ryan, D.E., Roy, S., Steinfeld, I., Lunstad, B.D., Park, J., Wilkens, A.B. et al. (2015) Chemically modified guide RNAs enhance CRISPR-Cas genome editing in human primary cells. *Nat. Biotechnol.*, **33**, 985–989.
61. Yin, H., Song, C.Q., Suresh, S., Wu, Q., Walsh, S., Rhym, L.H., Mintzer, E., Bolukbasi, M.F., Zhu, L.J., Kauffman, K. et al. (2017) Structure-guided chemical modification of guide RNA enables potent non-viral in vivo genome editing. *Nat. Biotechnol.*, **35**, 1179–1187.
62. McMahon, M.A., Prakash, T.P., Cleveland, D.W., Bennett, C.F. and Rahdar, M. (2018) Chemically modified Cpf1-CRISPR RNAs mediate efficient genome editing in mammalian cells. *Mol. Ther.*, **26**, 1228–1240.
63. Wu, H., Liu, Q., Shi, H., Xie, J., Zhang, Q., Ouyang, Z., Li, N., Yang, Y., Liu, Z., Zhao, Y. et al. (2018) Engineering CRISPR/Cpf1 with tRNA promotes genome editing capability in mammalian systems. *Cell Mol. Life Sci.*, doi:10.1007/s00018-018-2810-3.
64. Doench, J.G., Hartenian, E., Graham, D.B., Tothova, Z., Hegde, M., Smith, I., Sullender, M., Ebert, B.L., Xavier, R.J. and Root, D.E. (2014) Rational design of highly active sgRNAs for CRISPR-Cas9-mediated gene inactivation. *Nat. Biotechnol.*, **32**, 1262–1267.
65. Doench, J.G., Fusi, N., Sullender, M., Hegde, M., Vaimberg, E.W., Donovan, K.F., Smith, I., Tothova, Z., Wilen, C., Orchard, R. et al. (2016) Optimized sgRNA design to maximize activity and minimize off-target effects of CRISPR-Cas9. *Nat. Biotechnol.*, **34**, 184–191.
66. Cui, Y., Xu, J., Cheng, M., Liao, X. and Peng, S. (2018) Review of CRISPR/Cas9 sgRNA design tools. *Interdiscip. Sci.*, **10**, 455–465.
67. Byrne, S.M., Ortiz, L., Mali, P., Aach, J. and Church, G.M. (2015) Multi-kilobase homozygous targeted gene replacement in human induced pluripotent stem cells. *Nucleic Acids Res.*, **43**, e21.
68. Vazquez, J.C., Nogues, C., Rucker, E.B. and Piedrahita, J.A. (1998) Factors affecting the efficiency of introducing precise genetic changes in ES cells by homologous recombination: tag-and-exchange versus the Cre-loxp system. *Transgenic Res.*, **7**, 181–193.
69. Paix, A., Folkmann, A., Goldman, D.H., Kulaga, H., Grzelak, M.J., Rasoloson, D., Paidemarry, S., Green, R., Reed, R.R. and Seydoux, G. (2017) Precision genome editing using synthesis-dependent repair of Cas9-induced DNA breaks. *Proc. Natl. Acad. Sci. U.S.A.*, **114**, E10745–E10754.
70. Ma, Y., Zhang, X., Shen, B., Lu, Y., Chen, W., Ma, J., Bai, L., Huang, X. and Zhang, L. (2014) Generating rats with conditional alleles using CRISPR/Cas9. *Cell Res.*, **24**, 122–125.
71. Quadros, R.M., Miura, H., Harms, D.W., Akatsuka, H., Sato, T., Redder, R., Richardson, G.P., Inagaki, Y., Sakai, D. et al. (2017) Easi-CRISPR: a robust method for one-step generation of mice carrying conditional and insertion alleles using long ssDNA donors and CRISPR ribonucleoproteins. *Genome Biol.*, **18**, 92.
72. Miyasaka, Y., Uno, Y., Yoshimi, K., Kunihiro, Y., Yoshimura, T., Tanaka, T., Ishikubo, H., Hiraoka, Y., Takemoto, N., Tanaka, T. et al. (2018) CLICK: one-step generation of conditional knockout mice. *BMC Genomics*, **19**, 318.
73. Dewari, P.S., Southgate, B., McCarten, K., Monogarov, G., O'Duibhir, E., Quinn, N., Tyrer, A., Leitner, M.C., Plumb, C., Kalantzaki, M. et al. (2018) An efficient and scalable pipeline for epitope tagging in mammalian stem cells using Cas9 ribonucleoprotein. *Elife*, **7**, e35069.
74. Hockemeyer, D., Soldner, F., Beard, C., Gao, Q., Mitalipova, M., DeKelver, R.C., Katibah, G.E., Amora, R., Boydston, E.A., Zeitler, B. et al. (2009) Efficient targeting of expressed and silent genes in human ESCs and iPSCs using zinc-finger nucleases. *Nat. Biotechnol.*, **27**, 851–857.
75. Hockemeyer, D., Wang, H., Kiani, S., Lai, C.S., Gao, Q., Cassady, J.P., Cost, G.J., Zhang, L., Santiago, Y., Miller, J.C. et al. (2011) Genetic engineering of human pluripotent cells using TALE nucleases. *Nat. Biotechnol.*, **29**, 731–734.
76. Zhu, Z., Verma, N., Gonzalez, F., Shi, Z.D. and Huangfu, D. (2015) A CRISPR/Cas-mediated selection-free knockin strategy in human embryonic stem cells. *Stem. Cell Rep.*, **4**, 1103–1111.
77. Matano, M., Date, S., Shimokawa, M., Takano, A., Fujii, M., Ohta, Y., Watanabe, T., Kanai, T. and Sato, T. (2015) Modeling colorectal cancer using CRISPR-Cas9-mediated engineering of human intestinal organoids. *Nat. Med.*, **21**, 256–262.
78. Schwank, G., Koo, B.K., Sasselli, V., Dekkers, J.F., Heo, I., Demircan, T., Sasaki, N., Boymans, S., Cuppen, E., van der Ent, C.K. et al. (2013) Functional repair of CFTR by CRISPR/Cas9 in intestinal stem cell organoids of cystic fibrosis patients. *Cell Stem Cell*, **13**, 653–658.
79. Lengner, C.J., Camargo, F.D., Hochedlinger, K., Welstead, G.G., Zaidi, S., Gokhale, S., Scholer, H.R., Tomilin, A. and Jaenisch, R. (2007) Oct4 expression is not required for mouse somatic stem cell self-renewal. *Cell Stem Cell*, **1**, 403–415.
80. Chang, T.H., Huang, H.Y., Hsu, J.B., Weng, S.L., Horng, J.T. and Huang, H.D. (2013) An enhanced computational platform for investigating the roles of regulatory RNA and for identifying functional RNA motifs. *BMC Bioinformatics*, **14**(Suppl. 2), S4.
81. Liu, Y., Han, X., Yuan, J., Geng, T., Chen, S., Hu, X., Cui, I.H. and Cui, H. (2017) Biallelic insertion of a transcriptional terminator via the CRISPR/Cas9 system efficiently silences expression of protein-coding and non-coding RNA genes. *J. Biol. Chem.*, **292**, 5624–5633.
82. Fiering, S., Epner, E., Robinson, K., Zhuang, Y., Telling, A., Hu, M., Martin, D.I., Enver, T., Ley, T.J. and Groudine, M. (1995) Targeted deletion of 5'HS2 of the murine beta-globin LCR reveals that it is not essential for proper regulation of the beta-globin locus. *Genes Dev.*, **9**, 2203–2213.
83. Nagy, A., Moens, C., Ivanyi, E., Pawling, J., Gertsenstein, M., Hadjantonakis, A.K., Pirity, M. and Rossant, J. (1998) Dissecting the role of N-myc in development using a single targeting vector to generate a series of alleles. *Curr. Biol.*, **8**, 661–664.

84. Jacks, T., Shih, T.S., Schmitt, E.M., Bronson, R.T., Bernards, A. and Weinberg, R.A. (1994) Tumour predisposition in mice heterozygous for a targeted mutation in Nf1. *Nat. Genet.*, **7**, 353–361.
85. Nagy, A. (2000) Cre recombinase: the universal reagent for genome tailoring. *Genesis*, **26**, 99–109.
86. Meier, I.D., Bernreuther, C., Tilling, T., Neidhardt, J., Wong, Y.W., Schulze, C., Streichert, T. and Schachner, M. (2010) Short DNA sequences inserted for gene targeting can accidentally interfere with off-target gene expression. *FASEB J.*, **24**, 1714–1724.
87. Kim, S.I., Matsumoto, T., Kagawa, H., Nakamura, M., Hirohata, R., Ueno, A., Ohishi, M., Sakuma, T., Soga, T., Yamamoto, T. *et al.* (2018) Microhomology-assisted scarless genome editing in human iPSCs. *Nat. Commun.*, **9**, 939.
88. Yusa, K. (2013) Seamless genome editing in human pluripotent stem cells using custom endonuclease-based gene targeting and the piggyBac transposon. *Nat. Protoc.*, **8**, 2061–2078.
89. Maruyama, M., Ichisaka, T., Nakagawa, M. and Yamanaka, S. (2005) Differential roles for Sox15 and Sox2 in transcriptional control in mouse embryonic stem cells. *J. Biol. Chem.*, **280**, 24371–24379.
90. Lo, C.A., Kays, L., Emran, F., Lin, T.J., Cvetkovska, V. and Chen, B.E. (2015) Quantification of protein levels in single living cells. *Cell Rep.*, **13**, 2634–2644.
91. Miquerol, L., Langille, B.L. and Nagy, A. (2000) Embryonic development is disrupted by modest increases in vascular endothelial growth factor gene expression. *Development*, **127**, 3941–3946.
92. Duda, K., Lonowski, L.A., Kofoed-Nielsen, M., Ibarra, A., Delay, C.M., Kang, Q., Yang, Z., Pruett-Miller, S.M., Bennett, E.P., Wandall, H.H. *et al.* (2014) High-efficiency genome editing via 2A-coupled co-expression of fluorescent proteins and zinc finger nucleases or CRISPR/Cas9 nickase pairs. *Nucleic Acids Res.*, **42**, e84.
93. Seki, A. and Rutz, S. (2018) Optimized RNP transfection for highly efficient CRISPR/Cas9-mediated gene knockout in primary T cells. *J. Exp. Med.*, **215**, 985–997.
94. Steyer, B., Bu, Q., Cory, E., Jiang, K., Duong, S., Sinha, D., Steltzer, S., Gamm, D., Chang, Q. and Saha, K. (2018) Scarless genome editing of human pluripotent stem cells via transient puromycin selection. *Stem Cell Rep.*, **10**, 642–654.
95. Brinkman, E.K., Kousholt, A.N., Harmsen, T., Leemans, C., Chen, T., Jonkers, J. and van Steensel, B. (2018) Easy quantification of template-directed CRISPR/Cas9 editing. *Nucleic Acids Res.*, **46**, e58.
96. Brinkman, E.K., Chen, T., Amendola, M. and van Steensel, B. (2014) Easy quantitative assessment of genome editing by sequence trace decomposition. *Nucleic Acids Res.*, **42**, e168.
97. Lin, S., Staahl, B.T., Alla, R.K. and Doudna, J.A. (2014) Enhanced homology-directed human genome engineering by controlled timing of CRISPR/Cas9 delivery. *Elife*, **3**, e04766.
98. Liang, X., Potter, J., Kumar, S., Ravinder, N. and Chesnut, J.D. (2017) Enhanced CRISPR/Cas9-mediated precise genome editing by improved design and delivery of gRNA, Cas9 nuclease, and donor DNA. *J. Biotechnol.*, **241**, 136–146.
99. Guo, Q., Mintier, G., Ma-Edmonds, M., Storton, D., Wang, X., Xiao, X., Kienzle, B., Zhao, D. and Feder, J.N. (2018) ‘Cold shock’ increases the frequency of homology directed repair gene editing in induced pluripotent stem cells. *Sci. Rep.*, **8**, 2080.
100. Komor, A.C., Kim, Y.B., Packer, M.S., Zuris, J.A. and Liu, D.R. (2016) Programmable editing of a target base in genomic DNA without double-stranded DNA cleavage. *Nature*, **533**, 420–424.
101. Gaudelli, N.M., Komor, A.C., Rees, H.A., Packer, M.S., Badran, A.H., Bryson, D.I. and Liu, D.R. (2017) Programmable base editing of A*T to G*C in genomic DNA without DNA cleavage. *Nature*, **551**, 464–471.
102. Komor, A.C., Zhao, K.T., Packer, M.S., Gaudelli, N.M., Waterbury, A.L., Koblan, L.W., Kim, Y.B., Badran, A.H. and Liu, D.R. (2017) Improved base excision repair inhibition and bacteriophage Mu Gam protein yields C:G-to-T:A base editors with higher efficiency and product purity. *Sci. Adv.*, **3**, eaao4774.
103. Miura, H., Gurumurthy, C.B., Sato, T., Sato, M. and Ohtsuka, M. (2015) CRISPR/Cas9-based generation of knockdown mice by intronic insertion of artificial microRNA using longer single-stranded DNA. *Sci. Rep.*, **5**, 12799.
104. Miura, H., Quadros, R.M., Gurumurthy, C.B. and Ohtsuka, M. (2018) Easi-CRISPR for creating knock-in and conditional knockout mouse models using long ssDNA donors. *Nat. Protoc.*, **13**, 195–215.
105. Arbab, M., Srinivasan, S., Hashimoto, T., Geijsen, N. and Sherwood, R.I. (2015) Cloning-free CRISPR. *Stem Cell Rep.*, **5**, 908–917.
106. Sheridan, R.M. and Bentley, D.L. (2016) Selectable one-step PCR-mediated integration of a degron for rapid depletion of endogenous human proteins. *BioTechniques*, **60**, 69–74.
107. Shy, B.R., MacDougall, M.S., Clarke, R. and Merrill, B.J. (2016) Co-incident insertion enables high efficiency genome engineering in mouse embryonic stem cells. *Nucleic Acids Res.*, **44**, 7997–8010.
108. Zhang, J.P., Li, X.L., Li, G.H., Chen, W., Arakaki, C., Botimer, G.D., Baylink, D., Zhang, L., Wen, W., Fu, Y.W. *et al.* (2017) Efficient precise knockin with a double cut HDR donor after CRISPR/Cas9-mediated double-stranded DNA cleavage. *Genome Biol.*, **18**, 35.
109. Yao, X., Wang, X., Hu, X., Liu, Z., Liu, J., Zhou, H., Shen, X., Wei, Y., Huang, Z., Ying, W. *et al.* (2017) Homology-mediated end joining-based targeted integration using CRISPR/Cas9. *Cell Res.*, **27**, 801–814.
110. Schwank, G. and Clevers, H. (2016) CRISPR/Cas9-mediated genome editing of mouse small intestinal organoids. *Methods Mol. Biol.*, **1422**, 3–11.
111. Fujii, M., Matano, M., Nanki, K. and Sato, T. (2015) Efficient genetic engineering of human intestinal organoids using electroporation. *Nat. Protoc.*, **10**, 1474–1485.
112. Suresh, B., Ramakrishna, S. and Kim, H. (2017) Cell-penetrating peptide-mediated delivery of Cas9 protein and guide RNA for genome editing. *Methods Mol. Biol.*, **1507**, 81–94.
113. Zuris, J.A., Thompson, D.B., Shu, Y., Guilinger, J.P., Bessen, J.L., Hu, J.H., Maeder, M.L., Joung, J.K., Chen, Z.Y. and Liu, D.R. (2015) Cationic lipid-mediated delivery of proteins enables efficient protein-based genome editing in vitro and in vivo. *Nat. Biotechnol.*, **33**, 73–80.
114. Hornung, V. and Latz, E. (2010) Intracellular DNA recognition. *Nat. Rev. Immunol.*, **10**, 123–130.
115. Kim, S., Kim, D., Cho, S.W., Kim, J. and Kim, J.S. (2014) Highly efficient RNA-guided genome editing in human cells via delivery of purified Cas9 ribonucleoproteins. *Genome Res.*, **24**, 1012–1019.
116. Gaj, T., Guo, J., Kato, Y., Sirk, S.J. and Barbas, C.F. 3rd. (2012) Targeted gene knockout by direct delivery of zinc-finger nuclease proteins. *Nat. Methods*, **9**, 805–807.
117. Liang, X., Potter, J., Kumar, S., Zou, Y., Quintanilla, R., Sridharan, M., Carte, J., Chen, W., Roark, N., Ranganathan, S. *et al.* (2015) Rapid and highly efficient mammalian cell engineering via Cas9 protein transfection. *J. Biotechnol.*, **208**, 44–53.
118. Wang, H., Yang, H., Shivalila, C.S., Dawlaty, M.M., Cheng, A.W., Zhang, F. and Jaenisch, R. (2013) One-step generation of mice carrying mutations in multiple genes by CRISPR/Cas-mediated genome engineering. *Cell*, **153**, 910–918.
119. Wang, W., Kutny, P.M., Byers, S.L., Longstaff, C.J., DaCosta, M.J., Pang, C., Zhang, Y., Taft, R.A., Buaas, F.W. and Wang, H. (2016) Delivery of Cas9 protein into mouse zygotes through a series of electroporation dramatically increases the efficiency of model creation. *J. Genet. Genomics*, **43**, 319–327.
120. Gong, H., Liu, M., Klomp, J., Merrill, B.J., Rehman, J. and Malik, A.B. (2017) Method for dual viral vector mediated CRISPR-Cas9 gene disruption in primary human endothelial cells. *Sci. Rep.*, **7**, 42127.
121. Cheshenko, N., Krougliak, N., Eisensmith, R.C. and Krougliak, V.A. (2001) A novel system for the production of fully deleted adenovirus vectors that does not require helper adenovirus. *Gene Ther.*, **8**, 846–854.
122. Mansouri, M., Bellon-Echeverria, I., Rizk, A., Ehsaei, Z., Cianciolo Cosentino, C., Silva, C.S., Xie, Y., Boyce, F.M., Davis, M.W., Neuhauss, S.C. *et al.* (2016) Highly efficient baculovirus-mediated multigene delivery in primary cells. *Nat. Commun.*, **7**, 11529.
123. Hindriksen, S., Bramer, A.J., Truong, M.A., Vromans, M.J.M., Post, J.B., Verlaan-Klink, I., Snippert, H.J., Lens, S.M.A. and Hadders, M.A. (2017) Baculoviral delivery of CRISPR/Cas9 facilitates efficient genome editing in human cells. *PLoS One*, **12**, e0179514.

124. Han, X., Liu, Z., Jo, M.C., Zhang, K., Li, Y., Zeng, Z., Li, N., Zu, Y. and Qin, L. (2015) CRISPR-Cas9 delivery to hard-to-transfect cells via membrane deformation. *Sci. Adv.*, **1**, e1500454.
125. D'Astolfo, D.S., Pagliero, R.J., Pras, A., Karthaus, W.R., Clevers, H., Prasad, V., Lebbink, R.J., Rehmann, H. and Geijsen, N. (2015) Efficient intracellular delivery of native proteins. *Cell*, **161**, 674–690.
126. Gaj, T., Staahl, B.T., Rodrigues, G.M.C., Limsirichai, P., Ekman, F.K., Doudna, J.A. and Schaffer, D.V. (2017) Targeted gene knock-in by homology-directed genome editing using Cas9 ribonucleoprotein and AAV donor delivery. *Nucleic Acids Res.*, **45**, e98.
127. Yin, H., Xue, W., Chen, S., Bogorad, R.L., Benedetti, E., Grompe, M., Kotliansky, V., Sharp, P.A., Jacks, T. and Anderson, D.G. (2014) Genome editing with Cas9 in adult mice corrects a disease mutation and phenotype. *Nat. Biotechnol.*, **32**, 551–553.
128. Xue, W., Chen, S., Yin, H., Tammela, T., Papagiannakopoulos, T., Joshi, N.S., Cai, W., Yang, G., Bronson, R., Crowley, D.G. *et al.* (2014) CRISPR-mediated direct mutation of cancer genes in the mouse liver. *Nature*, **514**, 380–384.
129. Sanchez-Rivera, F.J., Papagiannakopoulos, T., Romero, R., Tammela, T., Bauer, M.R., Bhutkar, A., Joshi, N.S., Subbaraj, L., Bronson, R.T., Xue, W. *et al.* (2014) Rapid modelling of cooperating genetic events in cancer through somatic genome editing. *Nature*, **516**, 428–431.
130. Roper, J., Tammela, T., Cetinbas, N.M., Akkad, A., Roghanian, A., Rickelt, S., Almqadadi, M., Wu, K., Oberli, M.A., Sanchez-Rivera, F. *et al.* (2017) In vivo genome editing and organoid transplantation models of colorectal cancer and metastasis. *Nat. Biotechnol.*, **35**, 569–576.
131. Ehrke-Schulz, E., Schiwon, M., Leitner, T., David, S., Bergmann, T., Liu, J. and Ehrhardt, A. (2017) CRISPR/Cas9 delivery with one single adenoviral vector devoid of all viral genes. *Sci. Rep.*, **7**, 17113.
132. Lau, C.H. and Suh, Y. (2017) In vivo genome editing in animals using AAV-CRISPR system: applications to translational research of human disease. *F1000Res*, **6**, 2153.
133. Cox, D.B., Platt, R.J. and Zhang, F. (2015) Therapeutic genome editing: prospects and challenges. *Nat. Med.*, **21**, 121–131.
134. Savic, N. and Schwank, G. (2016) Advances in therapeutic CRISPR/Cas9 genome editing. *Transl. Res.*, **168**, 15–21.
135. Chu, V.T., Weber, T., Wefers, B., Wurst, W., Sander, S., Rajewsky, K. and Kuhn, R. (2015) Increasing the efficiency of homology-directed repair for CRISPR-Cas9-induced precise gene editing in mammalian cells. *Nat. Biotechnol.*, **33**, 543–548.
136. Maruyama, T., Dougan, S.K., Truttmann, M.C., Bilate, A.M., Ingram, J.R. and Ploegh, H.L. (2015) Increasing the efficiency of precise genome editing with CRISPR-Cas9 by inhibition of nonhomologous end joining. *Nat. Biotechnol.*, **33**, 538–542.
137. Vartak, S.V. and Raghavan, S.C. (2015) Inhibition of nonhomologous end joining to increase the specificity of CRISPR/Cas9 genome editing. *FEBS J.*, **282**, 4289–4294.
138. Li, G., Zhang, X., Zhong, C., Mo, J., Quan, R., Yang, J., Liu, D., Li, Z., Yang, H. and Wu, Z. (2017) Small molecules enhance CRISPR/Cas9-mediated homology-directed genome editing in primary cells. *Sci. Rep.*, **7**, 8943.
139. Hu, Z., Shi, Z., Guo, X., Jiang, B., Wang, G., Luo, D., Chen, Y. and Zhu, Y.S. (2018) Ligase IV inhibitor SCR7 enhances gene editing directed by CRISPR-Cas9 and ssODN in human cancer cells. *Cell Biosci.*, **8**, 12.
140. Kulkarni, S.S. and Canto, C. (2015) The molecular targets of resveratrol. *Biochim. Biophys. Acta*, **1852**, 1114–1123.
141. Ma, X., Chen, X., Jin, Y., Ge, W., Wang, W., Kong, L., Ji, J., Guo, X., Huang, J., Feng, X.H. *et al.* (2018) Small molecules promote CRISPR-Cpf1-mediated genome editing in human pluripotent stem cells. *Nat. Commun.*, **9**, 1303.
142. Xiang, G., Zhang, X., An, C., Cheng, C. and Wang, H. (2017) Temperature effect on CRISPR-Cas9 mediated genome editing. *J. Genet. Genomics*, **44**, 199–205.
143. Bobadilla, J.L., Macek, M. Jr., Fine, J.P. and Farrell, P.M. (2002) Cystic fibrosis: a worldwide analysis of CFTR mutations—correlation with incidence data and application to screening. *Hum. Mutat.*, **19**, 575–606.
144. Nagasaki, A., S.T.K., Yumoto, T., Imaizumi, M., Yamagishi, A., Kim, H., Nakamura, C. and T.Q.P.U. (2017) The Position of the GFP Tag on Actin Affects the Filament Formation in Mammalian Cells. *Cell Struct. Funct.*, **42**, 131–140.
145. Cranfill, P.J., Sell, B.R., Baird, M.A., Allen, J.R., Lavagnino, Z., de Gruiter, H.M., Kremers, G.J., Davidson, M.W., Ustione, A. and Piston, D.W. (2016) Quantitative assessment of fluorescent proteins. *Nat. Methods*, **13**, 557–562.
146. Clevers, H. (2016) Modeling development and disease with organoids. *Cell*, **165**, 1586–1597.
147. Shimokawa, M., Ohta, Y., Nishikori, S., Matano, M., Takano, A., Fujii, M., Date, S., Sugimoto, S., Kanai, T. and Sato, T. (2017) Visualization and targeting of LGR5(+) human colon cancer stem cells. *Nature*, **545**, 187–192.
148. Lee, K., Mackley, V.A., Rao, A., Chong, A.T., Dewitt, M.A., Corn, J.E. and Murthy, N. (2017) Synthetically modified guide RNA and donor DNA are a versatile platform for CRISPR-Cas9 engineering. *Elife*, **6**, e25312.
149. Carlson-Stevermer, J., Abdeen, A.A., Kohlenberg, L., Goedland, M., Molugu, K., Lou, M. and Saha, K. (2017) Assembly of CRISPR ribonucleoproteins with biotinylated oligonucleotides via an RNA aptamer for precise gene editing. *Nat. Commun.*, **8**, 1711.
150. Veneziano, R., Shepherd, T.R., Ratanalert, S., Bellou, L., Tao, C. and Bathe, M. (2018) In vitro synthesis of gene-length single-stranded DNA. *Sci. Rep.*, **8**, 6548.